

The Functional Organization and Cortical Connections of Motor Cortex in Squirrels

Dylan F. Cooke¹, Jeffrey Padberg², Tony Zahner^{1,3} and Leah Krubitzer^{1,3}

¹Center for Neuroscience, University of California, Davis, Davis, CA 95618, USA, ²Department of Biology, University of Central Arkansas, Conway, AR 72035, USA and ³Department of Psychology, University of California, Davis, Davis, CA 95618, USA

Address correspondence to Leah Krubitzer, Center for Neuroscience, University of California, Davis, 1544 Newton Court, Davis, CA 95618, USA. Email: lakrubitzer@ucdavis.edu.

Despite extraordinary diversity in the rodent order, studies of motor cortex have been limited to only 2 species, rats and mice. Here, we examine the topographic organization of motor cortex in the Eastern gray squirrel (*Sciurus carolinensis*) and cortical connections of motor cortex in the California ground squirrel (*Spermophilus beecheyi*). We distinguish a primary motor area, M1, based on intracortical microstimulation (ICMS), myeloarchitecture, and patterns of connectivity. A sensorimotor area between M1 and the primary somatosensory area, S1, was also distinguished based on connections, functional organization, and myeloarchitecture. We term this field 3a based on similarities with area 3a in nonrodent mammals. Movements are evoked with ICMS in both M1 and 3a in a roughly somatotopic pattern. Connections of 3a and M1 are distinct and suggest the presence of a third far rostral field, termed "F," possibly involved in motor processing based on its connections. We hypothesize that 3a is homologous to the dysgranular zone (DZ) in S1 of rats and mice. Our results demonstrate that squirrels have both similar and unique features of M1 organization compared with those described in rats and mice, and that changes in 3a/DZ borders appear to have occurred in both lineages.

Keywords: evolution, M1, primate, rodent, 3a

Introduction

Rodents are the most diverse order of mammals, varying along a variety of dimensions including body size, means of locomotion and navigation, peripheral morphology, relative brain size, diel pattern, terrain niche, and sociality (see Krubitzer et al. 2011). Rodentia comprises 5 suborders and 34 families and represents 40% (2277 species) of all mammalian species (Fig. 1). Despite this diversity, almost everything we know about rodent cortex organization, and much of what we know of mammalian brains, comes from 2 rodent species of the subfamily Murinae, mice and rats (Manger et al. 2008). These species share many aspects of neocortex organization, and these similarities are due not only to phylogeny but also due to similar morphological specialization (vibrissae), exploratory and navigation behaviors (whisking), diel pattern, locomotion, and terrain niche. As studied, both species are also reared in a highly deprived laboratory environment, and this in turn likely affects sensory and motor system development as well as the cortical phenotype (Campi et al. 2011). A critical problem of limiting studies of sensory and motor cortex to laboratory rats and mice is that the results cannot be generalized easily to other rodents, other mammals, and may not even be an accurate reflection of wild conspecifics.

Given the diversity in the rodent order, it is critical to explore the organization of motor cortex (M1, see Table 1 for abbreviations) in a variety of species to appreciate the general pattern of M1 organization in rodents and how that plan has

been modified to accommodate different lifestyles and behaviors. These data are also crucial for understanding general principles of mammalian brain evolution because they will elucidate the types of modifications that underlie adaptive, often complex, behaviors in mammals. Such changes are, of course, accompanied by alterations in patterns of connectivity that subserve these behaviors. For example, if motor and visual cortex coevolve with diel pattern and locomotive behaviors, one might expect to see connections between motor cortex and posterior parietal cortex (PPC) and/or visual cortex, much like that observed in other highly visual mammals such as tree shrews and primates (e.g., Fang et al. 2005; Remple et al. 2007). To date, studies of the topographic organization of motor cortex have been limited to rats (e.g., Hall and Lindholm 1974; Donoghue and Wise 1982; Neafsey et al. 1986; Tandon et al. 2008) and mice (Tennant et al. 2011). Using intracortical microstimulation (ICMS), these studies demonstrate that murine motor cortex has a roughly somatotopic organization with the hindlimb represented caudomedially and the forelimb lateral to this. Portions of the face such as the vibrissae representation are in a rostral or rostromedial location, while the jaw, lips, and tongue are represented rostrolaterally. Most studies in rats and mice have also described an additional rostral forelimb area/representation (RFA; Neafsey and Sievert 1982; Kleim et al. 1998; Brecht et al. 2004), but there is uncertainty as to whether this is a portion of M1 proper or a separate field. Cortex rostral to the primary somatosensory cortex has been divided into 2 architectonically distinct regions of cortex termed the lateral and medial agranular areas (AGl and AGm, respectively), but there is some debate on how the functionally defined motor fields correspond to these regions (see Discussion).

There were 3 goals of the present investigation. The first was to examine the functional organization in motor cortex in a rodent other than the mouse or rat to extend our understanding of rodent motor cortex organization. We chose the Eastern gray or tree squirrel, a member of the family Sciuridae, because they have a radically different lifestyle than that of mice and rats including a diurnal diel pattern, behavior, and morphology placing a greater emphasis on vision and varied terrain niches (tree squirrels are arboreal vs. the terrestrial Muridae) to name a few. Equally important is that our squirrels are wild caught, and thus, their sensory and motor systems developed in a much more complex environment than their laboratory-reared cousins.

Our second goal was to explore the intriguing possibility that rodents may have a sensorimotor area homologous to area 3a as described in other mammals. This possibility was first raised in early electrophysiological studies in rats, in which subdivisions of S1, including the rostrally located transitional zone (TZ), were postulated to be similar or homologous to area

Rodent Phylogeny

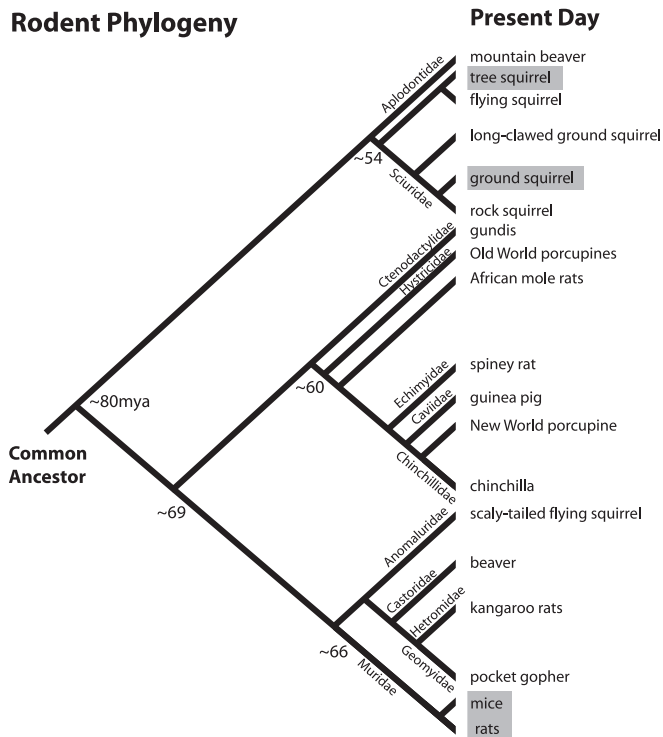


Figure 1. Phylogeny of the order Rodentia with representative individuals of different families listed. To date, studies of rodent motor cortex organization have been limited to rats and mice. The present investigation examines cortical organization and connections of a different rodent family, Sciuridae. Times of divergence are in millions of years ago (mya). Modified from Huchon et al. (2002, 2007) and Steppan et al. (2004).

3a (Chapin and Lin 1984). These data are complimented by more recent electrophysiological recording data in ground squirrels, in which a representation of deep receptors of the body was described and proposed to be homologous to area 3a (Slutsky et al. 2000). Finally, a comprehensive architectonic study in tree squirrels described a histologically distinct area between S1 and M1 that the investigators propose to be similar to area 3a in nonrodent mammals (Wong and Kaas 2008). Thus, accumulating evidence indicates that there is a distinct region between S1 and M1 in rodents that may be homologous to area 3a in nonrodent mammals.

Our third goal was to describe the cortical connections of motor cortex and a sensorimotor region just caudal to M1 and rostral to the primary somatosensory area (S1), the presumptive area 3a. We performed connectional studies in California ground squirrels. Studies of cortical connections of M1 have been described for mice and rats, but as with functional organization, nothing is known about patterns of connectivity for motor cortex in other rodents. We hypothesized that there would be some similarities to mice and rats in both topographic organization and connection patterns due to phylogeny, but there may also be differences associated with the coevolution of expanded visual cortex and visuomotor abilities in squirrels.

Materials and Methods

The functional organization of motor cortex was examined in 4 adult wild-caught Eastern gray squirrels (*Sciurus carolinensis*), commonly referred to as tree squirrels, with an average weight of 670 g (range 570–850 g). The connections of M1 and adjacent cortex were

examined in 5 (4 males and 1 female) wild-caught California ground squirrels (*Spermophilus beecheyi*; cases CGS1–5) with an average weight of 700 g (550–800 g). Although it was not possible to determine the age of these squirrels, the body weights and sizes indicated that they were all adults.

Dense ICMS mapping data in 4 tree squirrels (cases TS1–4) were related to myeloarchitectonic distinctions in tangentially sectioned cortex. Cortical connections in 5 ground squirrels were related to limited ICMS, electrophysiological recording, and myeloarchitecture (Table 2). Conceived and conducted as 2 separate studies, the data from these 2 species have been combined here since each informs the interpretation of the other. The use of these squirrel species for different aspects of this project was driven in part by anesthetic methodology. In the course of these studies, we found that functional mapping in the tree squirrel under our anesthetic protocol was effective in that movements could be evoked at low currents and experiments lasted long enough to generate detailed functional maps. However, these same methodologies were not as successful in the California ground squirrel. Anesthetic effects on motor mapping data have been recently described for rats by Tandon et al. (2008).

In the California ground squirrel experiments, we used long-duration stimulation and obtained relatively few stimulation sites for each case. However, these data were collected in the same animals that received injections of anatomical tracers and were valuable in helping us to interpret our connectional data. The tree squirrel is closely related to the California ground squirrel, and comparisons of the limited versus the dense mapping in the 2 species demonstrate that the maps appear to be quite similar.

Cortical injection locations of anatomical tracers were confirmed postmortem with cortical myeloarchitecture. When possible (4 of 5 cases), electrophysiological sensory mapping and/or ICMS results were related to injection sites and patterns of connections just prior to euthanasia (cases CGS1 and 4) or just prior to injection placement (CGS2 and 5). In case CGS3, tracers were injected in S1 using stereotaxic coordinates based on previous cases, but no functional mapping data were collected. Experimental protocols were approved by the Institutional Animal Care and Use Committee of the University of California, Davis and conformed to National Institute of Health guidelines.

Surgery and Neuroanatomical Tracer Injections

Standard sterile surgical procedures were followed in all cases. Ground squirrels were anesthetized with isoflurane gas (1–2% in O₂). Isoflurane reduced or eliminated ICMS movements, so for cases in which ICMS motor maps were used to place injections, an intramuscular (IM) injection of ketamine hydrochloride (30 mg/kg) and either xylazine (3 mg/kg) or medetomidine (0.03 mg/kg) was given. Dexamethasone (2 mg/kg, IM) was also administered to reduce inflammation. Additional doses of ketamine hydrochloride and xylazine or medetomidine were administered as needed to maintain a surgical level of anesthesia. In one case (CGS4), mapping was conducted under urethane anesthesia (1.25 g/kg, intraperitoneal). Subcutaneous injections of lactated Ringers solution (10 mL/kg/h) were made periodically. Approximately 0.1 cc of 2% lidocaine HCl was injected subcutaneously near the ear canals where the ear bars were to be inserted and at the scalp along the midline. The animal was then placed in a stereotaxic device with a custom-made mouthpiece that allowed us to deliver isoflurane, and later in the experiment (when we switched to ketamine), to observe face and mouth movements evoked with microstimulation. The scalp was cut along the midline and a craniotomy was performed over motor and somatosensory cortex. The dura was cut and folded away from the cortex, and the brain was kept moist with sterile saline. The brain was digitally imaged and electrode penetrations and injection locations were marked relative to the pattern of vasculature on this image.

A Hamilton syringe was used to inject 0.3 μL of 10% fluororuby (FR), 10% fluoroemerald (FE), or 10% biotinylated dextran amine (BDA). Eleven injections were placed in and restricted primarily to 1 of 4 areas: 3 in F, 3 in M1, 2 in 3a, and 3 in S1. Among these 11 injections, one was centered in M1 but spread slightly into cingulate cortex. Following the injections, a sterile soft contact lens was placed under the dura, and the flaps of the cut dura were laid on top of the lens. The craniotomy was covered with a cap made of dental acrylic and the skin was sutured. The

Table 1
Abbreviations

Cortical areas

A1	Primary auditory area
AGl	Lateral agranular field
AGm	Medial agranular field
cing	Cingulate cortex
DZ	Dysgranular zone
ER	Entorhinal cortex
F	Frontal myelinated area
M1	Primary motor area
OTc	Occipital temporal caudal area
OTr	Occipital temporal rostral area
PM	Parietal medial area (also referred to as PP)
PP	Posterior parietal cortex (previously referred to as PM)
PR	Parietal rhinal area
PV	Parietal ventral area
Pyr	Pyramidal cortex
R	Rostral auditory area
S1	Primary somatosensory area (cutaneous)
S2	Second somatosensory area
SMA	Supplementary motor area
TA	Temporal anterior area
TP	Temporal posterior area
TZ	Transitional zone
V1	Primary visual area
V2	Second visual area
3a	Somatosensory area (deep)
Body part representations/movements	
A	Ankle
Dig/D1-5	Digits 1-5
E	Elbow
Er	Ear
F	Face
FL	Forelimb
HL	Hindlimb
J	Jaw
K	Knee
L/Lid	Eyelid
LL	Lower lip
LT	Lower trunk
N	Naris
P1,2	Pads 1,2 (On glabrous forepaw)
SH	Shoulder
SN	Snout
T1-5	Toes 1-5
TR	Trunk
UL	Upper lip
UT	Upper trunk
V/Vib	Vibrissae
W	Wrist
Anatomical directions	
dor	Dorsal
v	Ventral
M	Medial
R	Rostral
Anatomical tracers	
BDA	Biotinylated dextran amine
DY	Diamidino yellow
FE	Fluoroemerald
FR	Fluororuby
Other	
ICMS	Intracortical microstimulation

animal was given analgesics (buprenorphine, 0.03 mg/kg, IM) and monitored closely before a terminal mapping procedure was carried out (2-7 days postoperatively).

Terminal Mapping

Following cortical injections and after tracers had been transported, sensory and motor properties of cortex were mapped in California ground squirrels. This surgery was similar to the first except for the following. Screws were inserted into the skull and cemented with dental acrylic to a bar to fix the head's position allowing ear bars and mouth holder to be removed to make observation of evoked movements easier. The craniotomy was enlarged and the exposed brain was covered in dimethylpolysiloxane to prevent desiccation. A digital image was made of the exposed cortex so that electrode stimulation sites could be marked relative to vasculature. Following mapping, selected recording sites were marked by reintroducing the electrode at those sites after it had been coated with 10% diamidino yellow (DY). Other sites were marked with electrolytic lesions (100- μ A 5-s DC pulse or 40- μ A 10-s DC pulse). Lesions and DY probes allowed us to relate functional data from specific recording and microstimulation sites to cortical field borders based on histological sections. We also performed terminal functional mapping experiments on tree squirrels, but these were not preceded by cortical injection experiments. Tree squirrels were given an IM injection of ketamine hydrochloride (30 mg/kg) and acepromazine (4.3 mg/kg). Maintenance doses of ketamine and acepromazine were given as needed to maintain a surgical level of anesthesia. Electrolytic lesions in tree squirrels used slightly different parameters than ground squirrels (10- μ A 10-s DC pulse).

Electrophysiological Recordings

In California ground squirrels, extracellular multiunit responses to somatosensory stimulation were obtained by lowering varnished tungsten microelectrodes (FHC, 0.25 mm diameter, 5 M Ω) 500-800 μ m perpendicularly into cortex with a micromanipulator (Kopf). The body surface was stimulated and neural activity was amplified, filtered, and monitored over a speaker. Cutaneous stimulation included displacement of hairs and light contact of the skin with a small paintbrush or a thin wooden probe. Deep receptors were stimulated with light taps to the skin, gentle manual squeezing, and passive joint rotation. For each recording site, receptive field extent was drawn on a picture of the body. The density of recording sites varied from case to case; the distance between penetrations ranged of 300-1000 μ m.

Intracortical Electrical Microstimulation

We used 2 different sets of stimulation parameters for the ICMS experiments, short-duration (40 ms) and long-duration (usually 500 ms but sometimes up to 800 ms) trains. The first was used in tree squirrels for motor cortex mapping, and the second was used in California ground squirrels for pre- or post hoc identification of our injection sites. Movements evoked with short-train stimulation were relatively simple, while those evoked with long-train stimulation were more complex. Both revealed similar roughly somatotopic organizations.

In the tree squirrels, stimulation was delivered through tungsten electrodes (1.5 M Ω at 1 kHz) and was generated by a 2-channel anapulse stimulator (WPI, Sarasota, FL) with 2 photon-coupled stimulus isolator units (WPI) operated in parallel. A ground screw was placed in

Table 2

Summary of experimental cases

Cases no	Injection site—tracer	ICMS mapping short train	Sensory mapping and ICMS mapping—long train
TS1 tree squirrel	None	M1, 3a (Fig. 4) ketamine/acepromazine	No
TS2 tree squirrel	None	M1, 3a (Fig. 5) ketamine/acepromazine	No
TS3 tree squirrel	None	M1, 3a (not shown) ketamine/acepromazine	No
TS4 tree squirrel	None	M1, 3a (not shown) ketamine/acepromazine	No
CGS1 ground squirrel	F-FE, F-FR (Not shown), 6.5-day survival	No	S1, 3a—Ketamine/xylazine
CGS2 ground squirrel	S1-FR, 3a-FE, 5-day survival	No	S1, 3a—ketamine/xylazine
CGS3 ground squirrel (Figs 2 and 3)	S1-FE, S1-FR, 2.2-day survival	No	No
CGS4 ground squirrel	M1-FE, F-FR, 5.3-day survival	No	S1, 3a, M1—urethane
CGS5 ground squirrel	M1-FR, 3a-FE, M1/cing-BDA, 7-day survival	No	M1, 3a—ketamine/xylazine no sensory mapping

the skull over visual cortex of the opposite hemisphere in tree squirrels; a needle placed in the dorsal neck muscle served as a ground in California ground squirrels. Constant currents were varied to determine the threshold for each stimulation site. The current levels were monitored on an oscilloscope by measuring the voltage drop across a resistor of known impedance in series with a stimulator circuit. Stimuli were biphasic, square wave, symmetric 0.5-ms pulses delivered at 300 Hz in 40-ms trains. Multiple densely spaced stimulation sites at depths of approximately 1000 μm were made throughout the exposed cortex. At each site, we started with an exploratory current of 100 μA and gradually decreased the current until threshold was reached. Threshold for these experiments was defined as the lowest current, for which a movement of a single muscle or body part could be evoked and observed by 2 experimenters. Microstimulation maps were related to histologically processed tissue with small electrolytic lesions made at selected stimulation sites.

In ground squirrels, long-duration stimulation trains were delivered immediately before or after sensory mapping at the same location and depth; therefore, a single electrode was used for both purposes. Neuronal responses could still be detected after long-duration super-threshold ICMS, suggesting that cortex was not adversely affected. A Grass S88 stimulator and 2 SIU6 stimulus isolation units (Grass, West Warwick, RI) generated a train of pulses, which were measured by the voltage drop across a 10 k Ω resistor in series with the return lead of the stimulation isolation units. We used parameters similar to those of other "long-duration" stimulation studies: a 500-ms train of biphasic 0.2-ms duration pulses at 200 Hz (Graziano et al. 2002; Stepniewska et al. 2005). If movements were not complete after 500 ms, the train was lengthened to as much as 800 ms. Current was initially set at 50 μA and was increased up to 150 μA if no movement was evoked at lower current levels. Movements evoked by stimulation were recorded on video, documented in writing, and drawn on an illustration of the animal.

Histological Processing

After time allowed for tracer transport (2–7 days) and following any terminal sensory or motor mapping, animals were administered a lethal dose of pentobarbital sodium (250 mg/kg) and transcardially perfused with 0.9% saline, followed by 4% paraformaldehyde in 0.1 M phosphate buffer (pH 7.4), and finally 4% paraformaldehyde in 10% phosphate-buffered sucrose. The brain was removed from the skull, and the cortical hemispheres were dissected from the rest of the brain and manually flattened between 2 glass slides. Flattened cortices were soaked overnight in phosphate buffer with 30% sucrose and then cut tangentially on a freezing microtome into 40- μm sections. This plane of section is widely used (e.g., Gould et al. 1986; Wang and Burkhalter 2007) and allowed us to relate a large cortical map to a small number of sections containing histological or connectional data. In this way, and particularly in lissencephalic brains, the 2D features of maps could be readily appreciated compared with standard planes of section. Alternate sections were stained for myelin (Fig. 2*D–F*; Fig. 3; Gallyas 1979) and, in cases with tracer injections, mounted for fluorescent microscopy (Fig. 2*A,B*) or reacted for BDA (Veenman et al. 1992; Vectastain Elite; Vector Laboratories, Burlingame, CA; Fig. 2*C*).

Data Analysis

Connectional data and marker probes were reconstructed using an imaging system composed of a fluorescent microscope attached to a computer equipped with optical plotting system software (MD Plot 5.2; AccuStage, Shoreview, MN). This system was used to plot the x - y coordinates of injection sites (Fig. 2*D*), the spread of the injection, retrogradely labeled cell bodies (Fig. 2*A–C*), marking lesions, and DY probes, as well as section outlines, blood vessels, and tissue artifacts. Myeloarchitectonic boundaries (Fig. 3) were drawn using a camera lucida and related to the x - y -plotted reconstruction by matching patterns of blood vessels and other features in adjacent sections. To facilitate the alignment of reconstructed sections with each other, minor distortions introduced to the tissue during histological processing and mounting were corrected by aligning corresponding blood vessels and thus digitally stretching or compressing the features of the

intervening tissue using the envelope mesh tool in Adobe Illustrator CS2. Myeloarchitecture and connectional data were related to sensory and motor mapping results by matching marking lesions and DY probes. In this way, the architectonic and functional boundaries of cortical fields could be compared with each other and could be used to identify the locations of injections and labeled connections. Although similar volumes of tracer were injected for all cases, differential uptake for the different tracers and cases produced different-sized injection sites. These differences in injection size and uptake were not related to differences in transport time.

Functional maps were reconstructed by demarcating groups of recording sites, at which neurons had similar receptive fields or movement fields. For each stimulation site, the movement was determined independently by 2 observers. For each tracer injection, the number of labeled cells in each field was counted, and relative connection strength was determined as follows. Cell counts for each field were divided by the total number of labeled cells in both hemispheres for each injection and for each hemisphere separately. This total count includes cells in the injected field except for cells inside the injection halo, where extracellular label indicates the extent of passive tracer spread. Because it was difficult to determine the exact boundary between the edge of the injection site and the beginning of dense intrinsic label, estimates of the density of intrinsic connections may be slightly under- or overestimated.

Results

We first describe our findings from short-duration ICMS experiments in tree squirrels from which detailed maps were obtained. Next, we describe the relationship of functional boundaries of sensory and motor cortical areas with myeloarchitectonic boundaries. Finally, we detail the ipsilateral and contralateral cortical connections of 4 areas of parietal and frontal cortex in 5 California ground squirrels: S1, 3a, M1, and F. These connections were related to myeloarchitectonic boundaries as well as functional boundaries of motor and somatosensory fields.

Topographic Organization of M1 Using Short-Duration Stimulation

Detailed maps using short-duration ICMS parameters of M1 were obtained in 2 tree squirrels, and partial maps were made in 2 tree squirrels (not shown). The currents needed to evoke movements ranged from 6 to 200 μA with a mean threshold of 34.6 μA for case TS1 (Fig. 4) and 25.8 μA for case TS2 (Fig. 5). As described in other mammals using similar techniques (Hall and Lindholm 1974; Gould et al. 1986; Neafsey et al. 1986; Tennant et al. 2011), there was a gross somatotopic organization in M1 with the hindlimb represented caudomedially, the forelimb represented lateral to this, and face and oral structures represented most rostrally within the representation (Figs 4 and 5). Within this gross pattern, however, the map was fractured such that movements of many body parts were represented in more than one location and adjacent stimulation sites often represented movements of nonadjacent body parts.

Several types of hindlimb movements were evoked at low thresholds including flexion, and more commonly, extension movements around the joints of the toes, ankle, and knee. The maps from cases TS1 and TS2 were generally similar, but one difference was the representation of the trunk, which was adjacent to the hindlimb in case TS1 (Fig. 4) but far rostrally in TS2 (Fig. 5, a single site). Further rostrally was a forelimb representation, including movements of the shoulder, elbow, wrist, and digits. The internal forelimb organization was fractured, except that in both cases, it was dominated by a central shoulder representation. Rostral to the forelimb was the

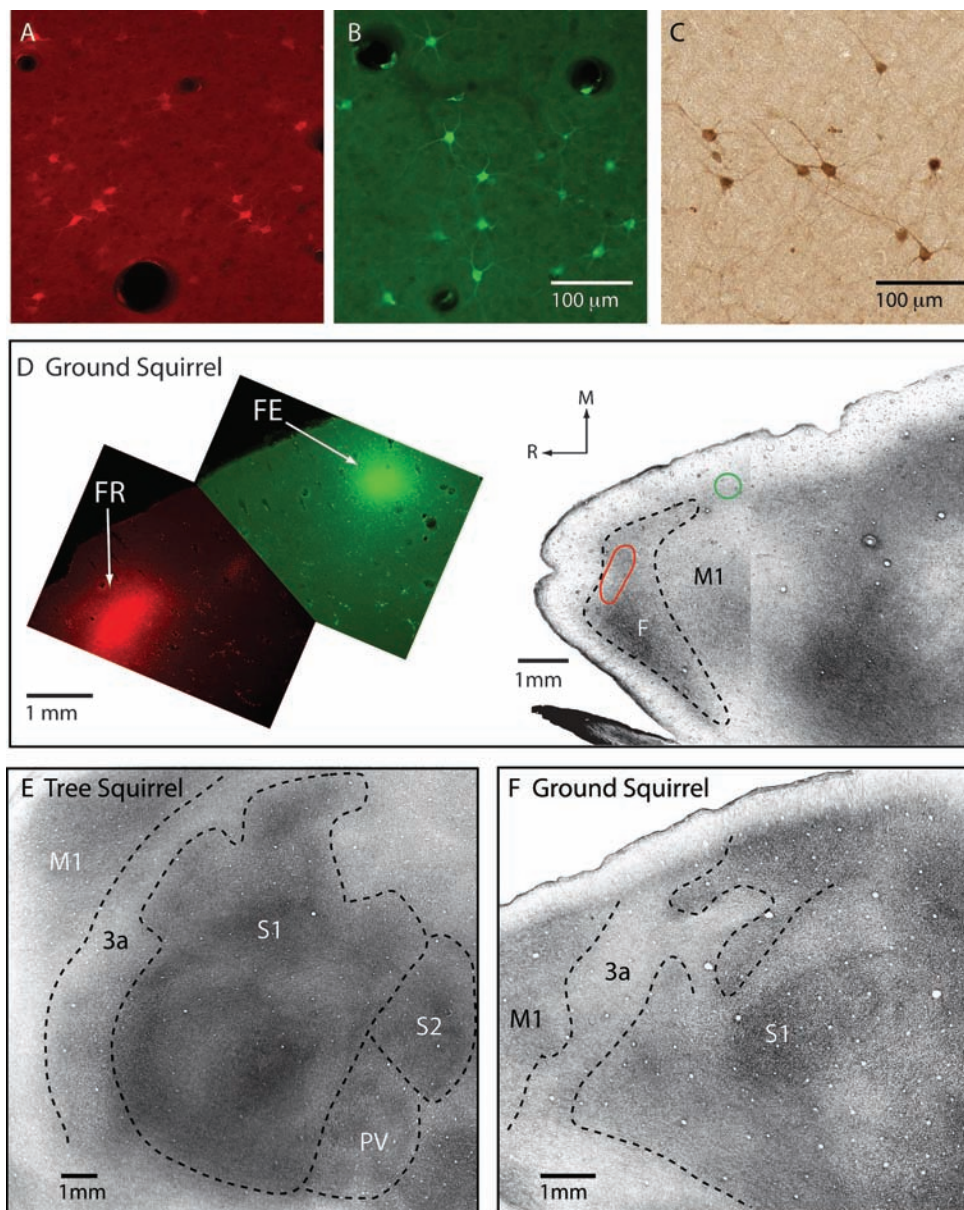


Figure 2. Digital images of retrogradely labeled cell bodies resulting from injections of FR (A) and FE (B) in S1 of case CGS3 and BDA (C) in M1 of case CGS4. The transported tracer almost completely filled labeled cells so that both the soma and some processes could easily be observed. (D) Injection sites of FR and FE injections in F and M1, respectively, in case CGS4. The locations of injections are shown on a composite image of myelin-stained cortex to the right in (D). All borders of all areas are not observed in a single section, but the darkly myelinated F is visible in this section as is the more moderately myelinated M1. Digital images of myelin-stained sections showing area 3a, S1, and portions of M1 in representative sections of the tree (E) and ground (F) squirrel. Area 3a stains lightly to moderately for myelin compared with S1. Although S1 in the ground squirrel (F) appears moderately myelinated at its rostralateral boundary, it becomes more heavily myelinated in deeper sections. Dashed lines indicate architectonic boundaries for this section and boundaries determined from adjacent sections. Although the entire series of sections was used to identify architectonic boundaries, many boundaries are often apparent in a single section. Rostral is left and medial is up. See Table 1 for other abbreviations.

bulk of the vibrissae representation, although particularly in case TS1, vibrissae movements could be elicited at multiple sites throughout M1. Vibrissae primarily depressed during stimulation. Within the vibrissae, representation of case TS1 was a region where blinks and eye and ear movements were evoked. A single blink site in the same position was observed in the less densely mapped case, TS2. Further rostral was a second forelimb representation, again including movements of the shoulder, elbow, wrist, and digits. In case TS1, movements restricted to digit 5 at one site and digits 4–5 at another site were also observed. Finally, furthest lateral (along with vibrissae sites) was

the remainder of the face representation, including the jaw, snout, and (in case TS2) buccal muscles.

For both cases in which detailed maps were generated, the face/oral structures and vibrissae comprised 54–63% of the representation of M1 plus 3a. Representations of the forelimb including the wrist/elbow, arm, and digits comprised 23–30% of the representation and the lower body representation comprised 4% of the representation. It should be noted that the far medial and far lateral extent of 3a and M1 were not fully explored so that portions of the hindlimb and face/oral representations may be underrepresented for each case.

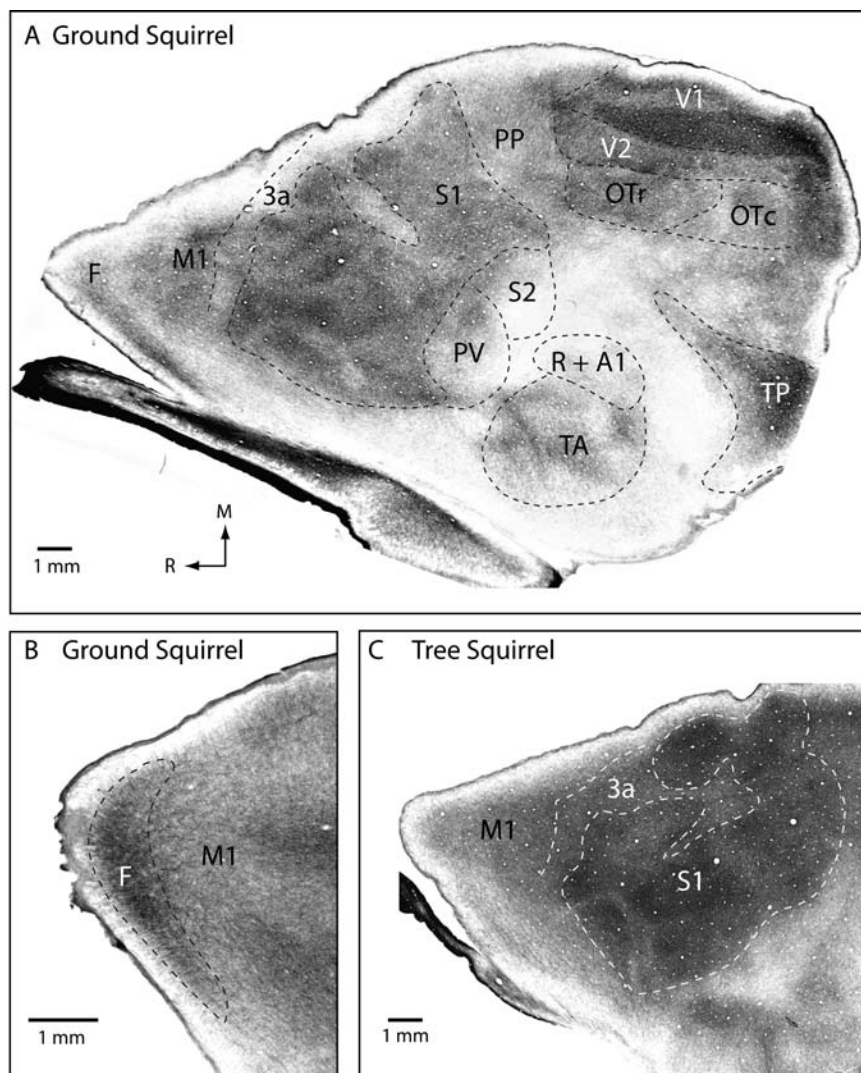


Figure 3. Tangentially sectioned myelin-stained cortex of California ground squirrels (A–B) and an Eastern gray squirrel or tree squirrel (C). While S1 is clearly distinct from rostral areas of cortex, in middle and deep layers, both areas 3a and M1 are moderately myelinated (C), compared with more superficial layers (compare with Fig. 2E). Conventions as in previous figures.

Although most movements evoked with these short-duration stimulation parameters were relatively simple and involved a single type of movement of one body part (e.g., arm rotation or vibrissae depression), in some instances, even at low thresholds (e.g., 7 μ A, case TS1), we evoked movements that incorporated multiple body parts such as forelimb lateral rotation and vibrissae depression. That is, movements of 2 or more body parts were represented at a single site and shared a current threshold. Multijoint movements from a single stimulation site sometimes spanned many disparate body parts, for example, the ankle, knee, trunk, and shoulder (15 μ A, case TS1). Percentages of various body parts within the map listed in the preceding paragraph do not include sites representing multiple body segments (mostly face or vibrissae plus forelimb), which accounted for 9–11% of total sites. The frontal area was not fully explored in tree squirrels using ICMS.

Cortical Myeloarchitecture

The myeloarchitecture of all of somatosensory cortex has been well described in previous studies in squirrels (e.g., Sur

et al. 1978; Krubitzer et al. 1986; Slutsky et al. 2000), and our results are similar to these previous studies. S1 was co-extensive with a darkly myelinated area that was segregated by myelin-light bands (Fig. 3A,B). These myelin-dense regions corresponded to major body part representations with the most prominent myelin-light band falling between the face/chin representation and the forelimb/forepaw representation. The poorly myelinated zone between these representations has been described in previous studies in squirrels using similar recording and/or architectonic techniques (Sur et al. 1978; Krubitzer et al. 1986; Slutsky et al. 2000; Wong and Kaas 2008). Immediately rostral to S1 was a more moderately myelinated strip of cortex that we and others (Wong and Kaas 2008) term area 3a (Figs 2 and 3). In middle and deeper layers, this area stains more darkly for myelin. This region was coextensive with a functional map of the body, in which neurons respond to stimulation of the muscles and joints of the contralateral body (Slutsky et al. 2000; Fig. 7B). Additionally, microstimulation at many sites in this region evoked body part movements (Figs 4 and 5).

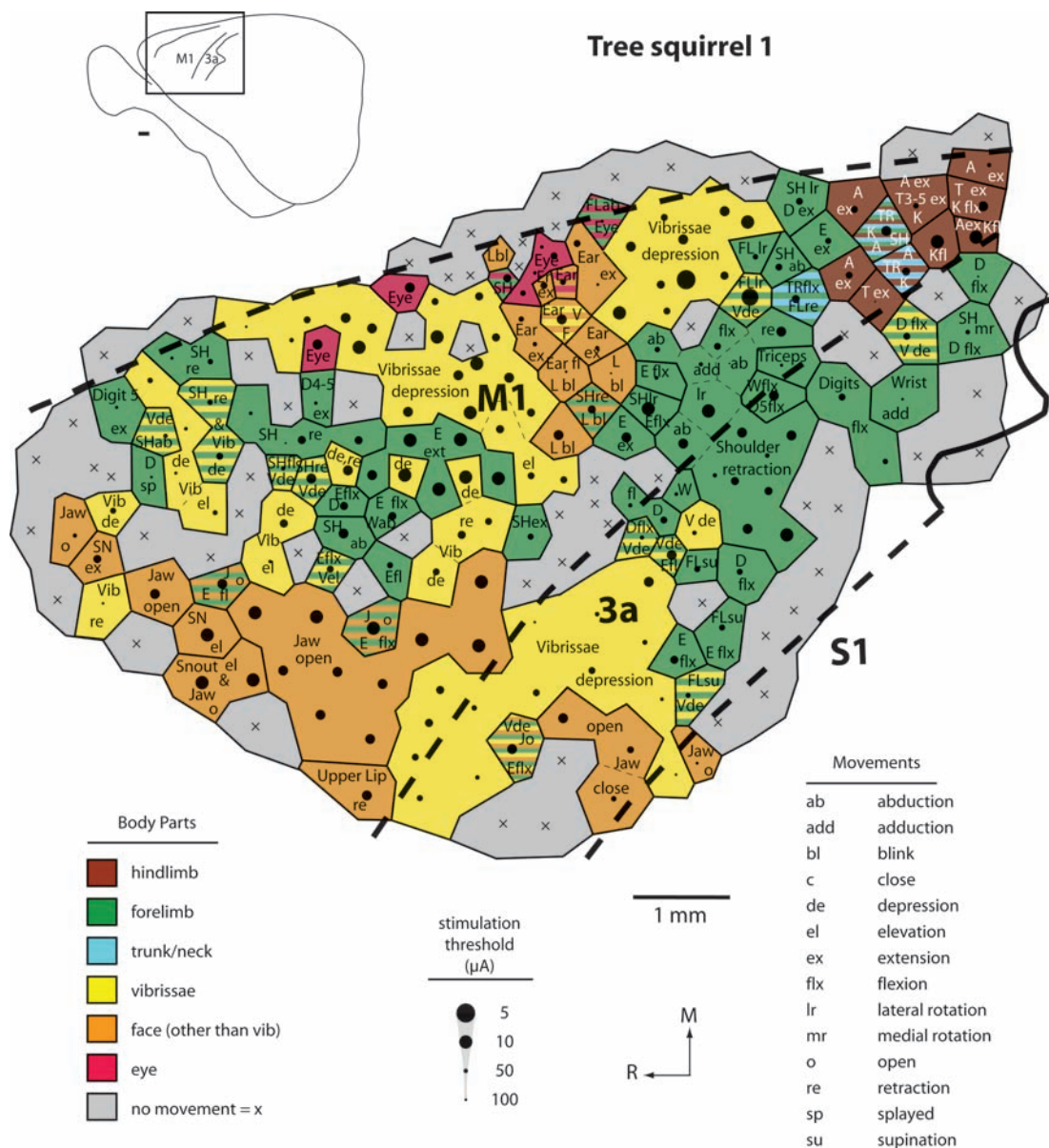


Figure 4. Functional map of movements evoked with short-duration threshold-level ICMS in a tree squirrel (case TS1). Borders based on myeloarchitecture and electrophysiology were aligned to functional maps using electrolytic lesions located at specific stimulation sites. Stimulation sites are marked with circles (evoked movement) or "X"s (no movement evoked). Circle diameter is inversely proportional to the measured current threshold. Colored polygons indicate what body part(s) moved consistently during threshold-level stimulation. Thin dashed lines separate different movements of the same body parts. In this figure, abbreviated body parts are capitalized and abbreviated movements are not. Map is left-right reversed for comparison with other cases.

Immediately rostral to area 3a was a moderately myelinated field, in which both long- and short-duration ICMS evokes body part movements (Figs 4, 5, and 6B). In superficial layers, this region stained lightly for myelin. This field was similar in location and appearance to AGI or M1 described in other rodent and other mammals. M1 in the squirrel was wedge shaped and occupied much of the frontal pole of dorsolateral cortex (Figs 3–6). In some cases, the rostromedial portion of M1 appeared slightly more myelinated, but this architectonic distinction did not appear to correspond to any functional distinctions.

At the rostral pole of dorsolateral frontal cortex, there was a thin, crescent-shaped, darkly myelinated area that was distinct from the moderately myelinated M1 located just caudally (Figs 2 and 3). We and other laboratories have termed

this area the frontal myelinated region, or F (Wong and Kaas 2008), although area F of Wong and Kaas appears somewhat larger in size than in the present study. Other subdivisions of parietal, occipital, and temporal cortex were readily identified (Fig. 3) and have been described previously in squirrels (e.g., Hall et al. 1971; Kaas et al. 1972; Merzenich et al. 1976; Luethke et al. 1988; Sereno et al. 1991; Slutsky et al. 2000; Wong and Kaas 2008; Campi and Krubitzer 2010).

Ipsilateral Cortical Connections of S1, 3a, M1, and F

In these experiments, different anatomical tracers were placed in different cortical fields in ground squirrels. When possible, injections were placed in functionally specified regions, but in

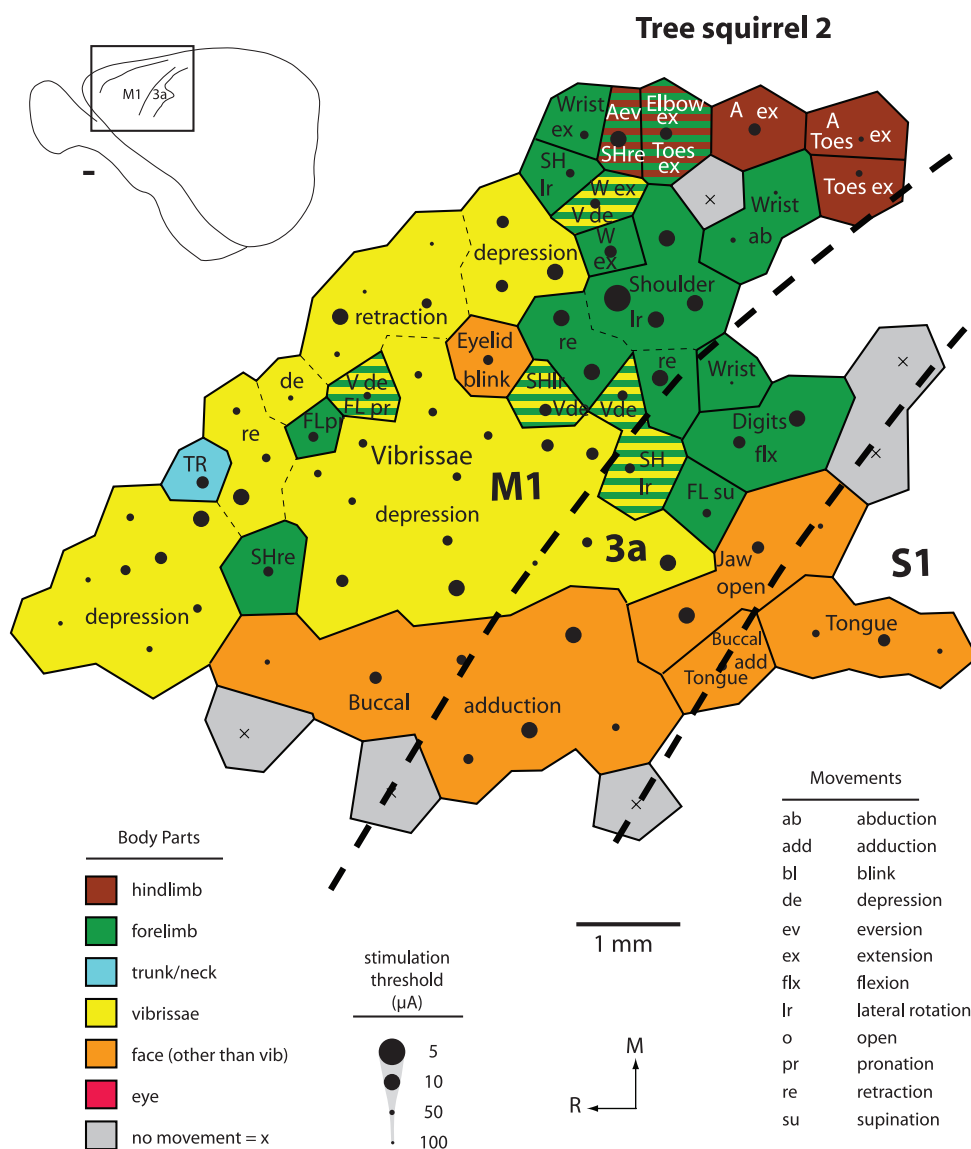


Figure 5. Functional map of movements evoked with short-duration threshold-level ICMS in an Eastern gray squirrel (case TS2). See Figure 4 for details. Estimated areal borders are shown as no myeloarchitecture was available for this case.

some instances, we could not consistently evoke movements under the anesthetic used for some of our chronic experiments (particularly isoflurane).

Functional Identification of Injection Sites and Resulting Label

As in previous studies in squirrels and other mammals (Sur et al. 1978; Kaas 1983; Krubitzer et al. 1986; Krubitzer and Disbrow 2008), neurons in ground squirrel primary somatosensory area, S1, responded to cutaneous stimulation of the contralateral body, with the chin, lips, and naris represented laterally in the field. The representation of the proximal forelimb and forepaw was medial to the face representation and the trunk was located further medial. The forepaw was represented at the rostral boundary of S1, the wrist was represented caudal to this, and the rest of the forelimb was represented medially (data not shown). Also, as previously described in our laboratory in ground squirrels (Slutsky et al. 2000), we identified a narrow strip of cortex immediately rostral to S1 that contained neurons that

required more intense stimulation of the contralateral body, such as muscle and joint manipulation. This field had a gross topographic organization with the chin and face represented most laterally in the field, the forelimb and forepaw represented medial to this, and a very small representation of the hindlimb in the medial-most portion of the field. Because current and previous data strongly indicate that this region is homologous to area 3a in other species such as monkeys, ferrets, and cats (see Discussion), we term this field area 3a. Somatic stimulation did not elicit a response in M1.

Effects of long-duration ICMS were tested at many of the same electrode sites, at which sensory responses were recorded (Figs 6 and 7). Observable muscle movements were evoked at depths of 1000–1500 μm . Although only a small number of sites were tested compared with short-duration ICMS in tree squirrels, we established that ICMS in both area 3a and M1 could evoke movements in anesthetized ground squirrels but not consistently. For a small proportion of sites in 3a in which somatic stimulation generated a neural response,

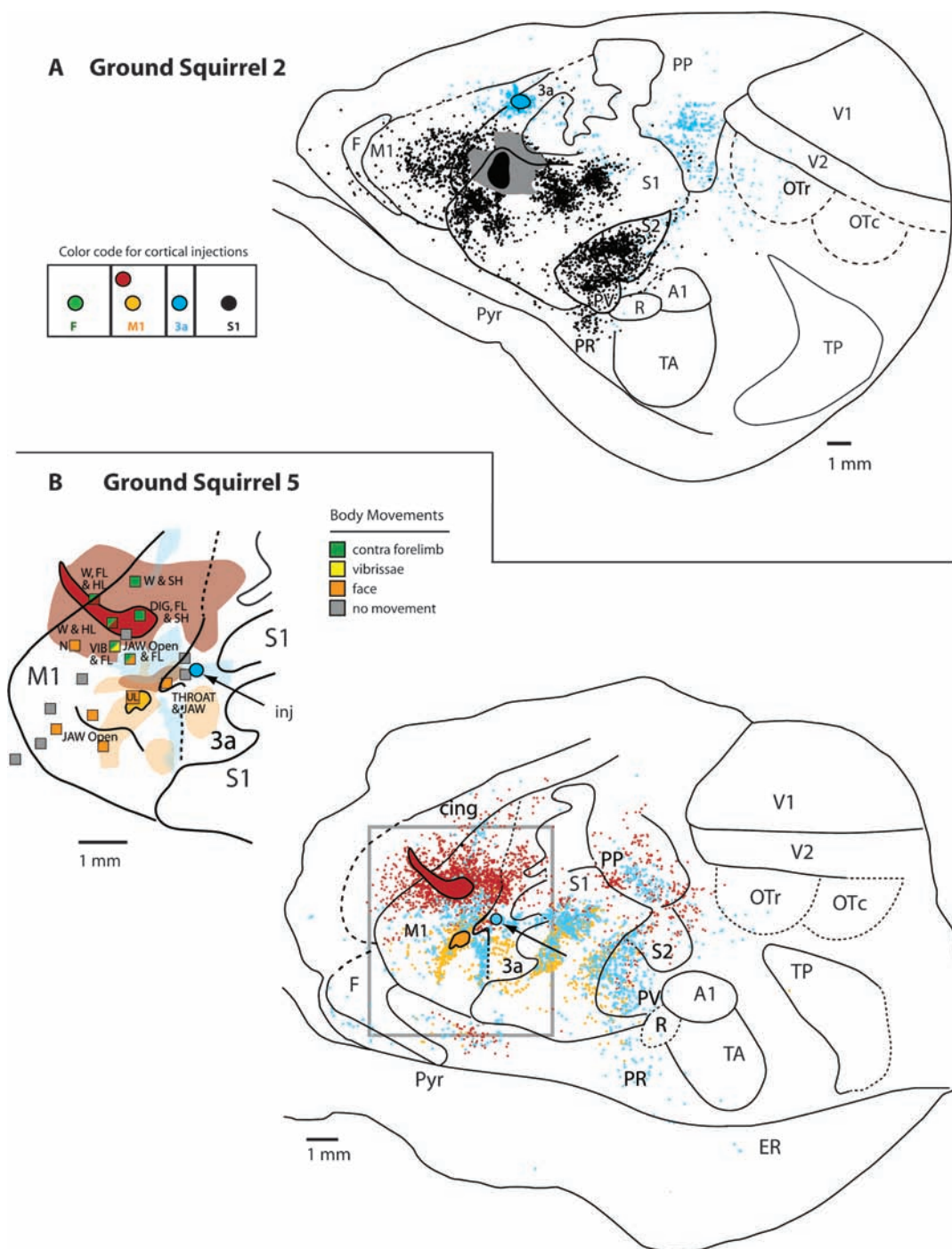


Figure 6. (A) Ipsilateral connections of S1 and 3a in case CGS2 and the relation of these general patterns of connections to architectonic boundaries. For ease of comparison across cases, injection sites and labeled cell bodies are colored according to injected field, not necessarily the tracer color (upper left box). The blue injection in area 3a is FE. The black injection in S1 is FR. (B) Ipsilateral connections of M1 and 3a in case CGS5 and the relation of these general patterns of connections to architectonic boundaries (bottom) and ICMS sites (top). The blue injection in area 3a (black arrow) is FE, the red injection in M1 is BDA, and the orange injection in M1 is FR. The large gray box in the bottom illustration shows the region detailed in the enlarged illustration above. The squares in the enlarged illustration indicate the locations tested with ICMS and are colored according to the body part(s) where movements were observed. In the enlarged ICMS-mapped region, patches of moderate to dense connections are colored according to the location of the corresponding injection. As in the case illustrated in (A), area 3a receives dense inputs from M1, S1, and PP. Sparse connections are observed with S2 and dense connections are observed with PV. The projections to area 3a appear to be from mediolaterally matched locations in S1. Connections with M1 are most dense with the vibrissae and mouth movement areas of M1 (B), but there are also connections with medial portions of M1 near the hindlimb representation. The connections of the more medial portion of M1, in the representation of the wrist extension and hindlimb movements (B) are with medial portions of 3a, F, and S1. However, the connections of M1 are less dense with S1 than are the connections of 3a. M1 also receives projections from PP and sparse projections from S2 and PV. Within M1, connections are with other movement representations of the forelimb and hindlimb as well as with mouth movement representations (B). The lateral injection in upper lip/vibrissae retraction representation in M1 has similar overall patterns of connections to the more medial injection, but the connections with S1 are denser, the connections with F are sparse, and no connections are observed with PP. Most of the intrinsic connections with M1 resulting from this injection site are with other representation of mouth, vibrissae, and face movements (B). Solid lines mark myeloarchitectonic borders and dashed black lines are approximate borders. Dots indicate individual retrogradely labeled cells from injection sites, and the extent of the injection site is marked as a solid color. Rostral is left; medial is up. Conventions as in previous figures. See Table 1 for abbreviations.

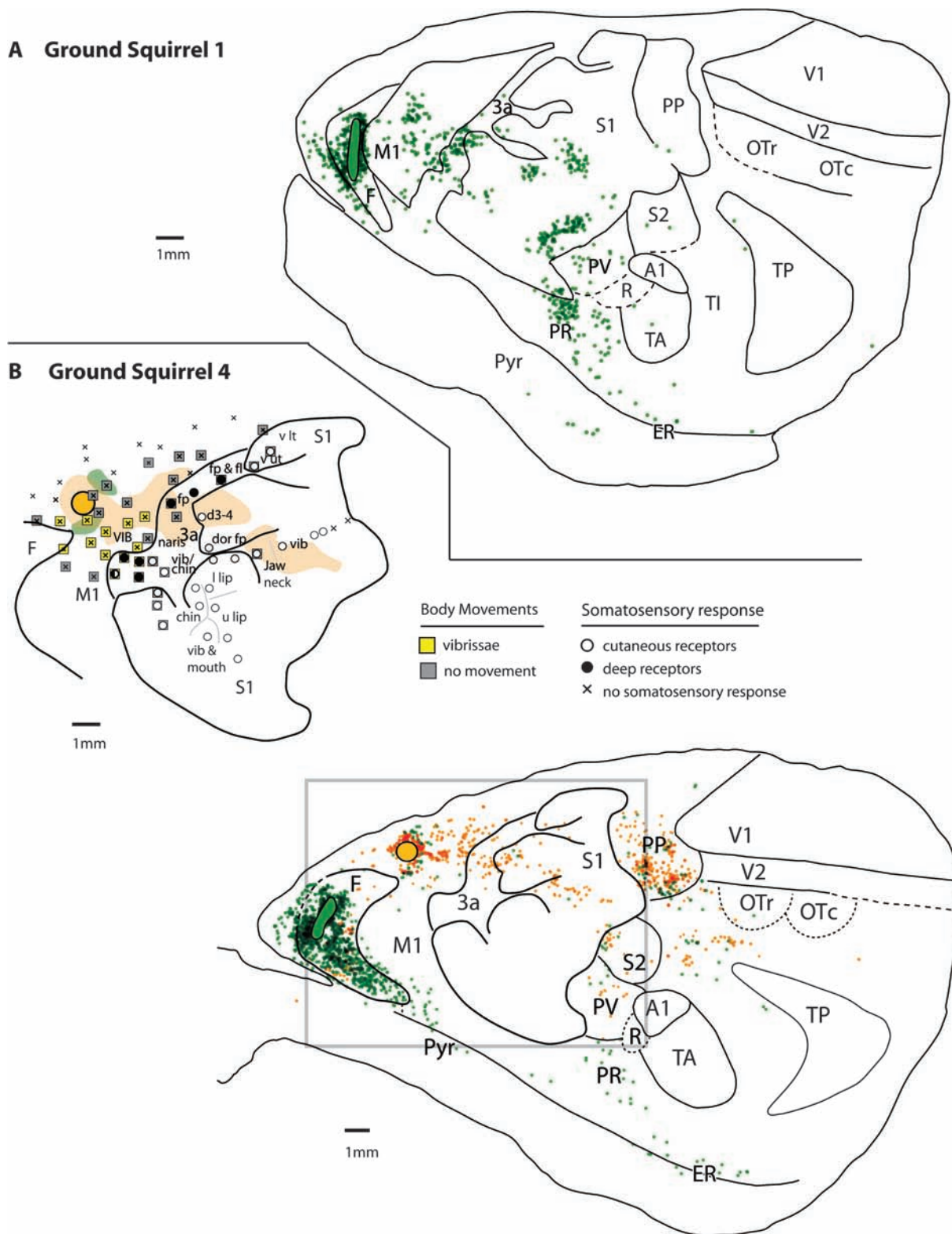


Figure 7. (A) Ipsilateral connections of F in case CGS1. In this case, FE was injected in a medial location (not shown), and FR was injected slightly more laterally in the same field. Since both injections yielded similar patterns of connections, only the lateral FE injection is illustrated here. Connections of F are most dense with M1, 3a, S1, PV, and PR. (B) Ipsilateral connections of M1 and F in case CGS4 (bottom) and the relation of these general patterns of connections to architectonic boundaries and ICMS sites (enlargement). The orange injection in M1 is FE and the green injection in F is FR. The connections of M1 are similar to those observed in case CGS5 (Fig. 6B), with differences mainly in the density of connections. Connections of cortical area F are distinct from those of M1 and are similar to those described for CGS1 illustrated in (A) with differences mainly in the density of connections. As shown in the enlarged map in (B), in this case, the injection in M1 was close to a vibrissae movement representation but may have invaded forelimb movement representations as well. The label resulting from this injection was found in the vibrissae movement representation in M1, the forepaw sensory representation in 3a, and the digit and vibrissae representation in S1. The label in M1 resulting from the injection in F was in the vibrissae movement representation and in cortex just medial to this (see Figs 4 and 5). Conventions as in previous figures. See Table 1 for abbreviations.

ICMS also generated movements (Cooke et al. 2008; cases not shown). In addition, somatic and motor fields overlapped such that when stimulation of deep receptors of the forelimb elicited a response in area 3a, ICMS at this same site produced forelimb movements. With the exception of a few sites bordering 3a, we did not generate movements from ICMS sites in S1 under our anesthetic conditions nor did we generate movements in F.

In M1, movements were evoked at many but not all sites (Figs 6 and 7), likely due to fluctuations in the anesthetic plane. As described in the previous section on short ICMS in the tree squirrel, at a gross level, M1 in ground squirrels is roughly somatotopically organized, with the forelimb represented medially and portions of the face represented laterally and rostrally (Fig. 6B). In the following section on connections, anatomical tracers and labeled cells are colored according to the area in which the injection was placed, rather than the color of the actual tracer.

Connections of S1

The pattern of cortical connections of S1 has been previously described in the Eastern gray squirrel, and the results presented here come from 3 injections into the face/lips representations in S1 in 2 California ground squirrels. In case CGS2, FR was injected in the rostralateral portion of S1 in the representation of the lower lip (Fig. 6A). In case CGS3 (not shown), in which no functional mapping took place, FR was injected in a similar lateral location to that in CGS2, and FE was injected just medial to the FR injection. As in the tree squirrel, a large number of patchy connections were observed intrinsically within other portions of the face and lips representations of S1 (Fig. 6A). Dense label was also observed rostrally with areas 3a and M1 at a mediolateral level similar to that injected in S1, and in S2, parietal ventral (PV), and parietal rhinal (PR). Sparse label was observed in the lateral portion of posterior parietal (PP), in F and in cortex just rostral to F. Finally, a few labeled cells were observed just lateral to S1 and caudal to S1. This overall pattern of label was similar for all S1 injections, although in some cases, injections were on the border of S1 and 3a. Cell counts, averaged across all cases, indicated the largest projections to S1 were from within S1 and from S2, PV, M1, and 3a in descending order. The remainder of label was found in other parts of ipsilateral cortex and in the contralateral hemisphere. It should be noted that label near the S1 injection site in case CGS2 (gray area near injection site in Fig. 6A) was so dense that cells in this region could not be accurately counted. Cell counts in this region, which includes part of S1 and 3a, were therefore understated, and consequently, percentage values of labeled cells in all other fields for this injection in this case, including callosal label in the opposite hemisphere in Figure 9A, were overstated.

Connections of Area 3a

In 2 squirrels, injections were limited to area 3a. In one of these (Fig. 6A), FE was injected into the medial portion of 3a. In the second case (Fig. 6B, arrow), FE was injected into a restricted portion in lateral 3a. In both cases, local connections were observed within area 3a, but these were relatively sparse. Dense projections were also observed with PP and moderate to dense connections were observed with S1, M1, and PV in descending order. Sparse label was observed in occipital temporal rostral, S2, PR, and in one case, a few cells were

observed just lateral to M1. Other parts of ipsilateral cortex and the contralateral hemisphere accounted for remaining label.

Projection patterns often included similar mediolateral locations in adjacent fields. For example, injections in the medial portion of area 3a resulted in labeled cells mainly with corresponding medial portions of M1 and S1 in cortex demonstrated to contain the representations of the forelimb and forepaw (e.g., Sur et al. 1978; Slutsky et al. 2000). However, there were also some labeled cells lateral to the lightly myelinated region in S1 that previous studies demonstrate divides the head and face laterally from the forelimb medially (e.g., Sur et al. 1978). Injections in the lateral portion of area 3a resulted in labeled cells in the lateral portion of S1, but label was also observed in the more lightly myelinated region of S1. Label in M1 was patchy and was found in the representation of vibrissae, mouth, and forelimb movements (Fig. 6B). Sparse label was also observed in far medial parts of M1.

Connections of M1

Three injections were placed in M1 in 2 squirrels (Figs 6B and 7B). Two of these injections were clearly limited to M1, and data from these cases (CGS4; CGS5, FR injection) were used to calculate average cell counts and percent of label (Fig. 9). In case CGS5, BDA was injected in a wrist extension/hindlimb movement representation of M1 but spread slightly into cingulate cortex (Fig. 6B). Of the 2 injections clearly restricted to M1, one was in the same case, CGS5, in which a small injection of FR was placed in an upper lip/vibrissae retraction representation of M1. In the second case, CGS4, FE was injected rostrally in M1, immediately adjacent to the vibrissae movement representation (Fig. 7B). Although the amount of label varied across cases due to differential uptake of tracer resulting in different size injections, in general, the overall patterns of connections were similar for all M1 injections. All injections in M1 resulted in dense intrinsic connections within M1. For the 2 cases in which ICMS/electrophysiological data were combined with connectional data (Figs 6B and 7B), we observed topographically matched and mismatched connections. Injections in the wrist extension/hindlimb movement representation resulted in intrinsic connections with other forelimb, wrist, and hindlimb movement representations. A small patch of label was also observed with a mouth movement representation (Fig. 6B). For the injection in the upper lip/vibrissae retraction representation, most label in M1 was associated with other mouth and oral structure movement representations; a small patch of labeled cells was also observed medially, near the wrist flexion/forearm movement representation (Fig. 6B). For the case in which the injection was placed immediately adjacent to the vibrissae movement representation (Fig. 7B), label in M1 was associated with other vibrissae movement representations, although label also spread medially.

Label in areas 3a and S1 for all injections was mostly found at similar mediolateral locations to injection sites in M1, but sparse label was found in other locations. For example, injections in the wrist extension/hindlimb representation in M1 resulted in label in the medial portion of 3a and S1, but sparse label in S1 was also observed somewhat laterally (Fig. 6B). In another example, the injection in the upper lip/vibrissae retraction representation in M1 resulted in label in the lateral portion of areas 3a and S1 where the face and lips have been reported to be represented (Sur et al. 1978). Finally, the injection near the vibrissae representation in M1 (but likely

involving portions of the forelimb representation as well) resulted in label in the forepaw representation in area 3a, the digit representation in S1, and the vibrissae representation in S1 (Fig. 7B).

Other areas that were labeled following injections in M1 included the lateral portion of PP, S2, PV, and extrastriate cortex. For 2 injections, label was observed in F. Other parts of ipsilateral cortex and the contralateral hemisphere accounted for remaining label.

Connections of F

Two injections were placed entirely within the frontal myelinated region F in 2 animals (Fig. 7A,B); case CGS4 received FR and case CGS1 received FE. One injection was in F and M1 combined and is not shown. We observed dense intrinsic connections, with some label also in cortex immediately rostral to area F. Moderate to sparse connections were observed with S1, M1, PR, 3a, PV, PP, entorhinal cortex, extrastriate cortex, pyriform cortex, and S2 in descending order. Other parts of ipsilateral cortex and the contralateral hemisphere accounted for remaining label.

Callosal Connections of S1, 3a, M1, and F

For all injections (except one BDA injection), labeled cells in the opposite hemisphere were observed and were directly related to myeloarchitectonic boundaries (Fig. 8). Percentages described here are of total callosal label averaged across all similar injections. Callosal connections of S1 were most dense with homotopic locations of S1 in the opposite hemisphere (Fig. 8A). Scattered labeled cells were also observed in nearby locations in S1. Labeled cells were also observed throughout the mediolateral extent of area 3a and in a location in M1 that matched the mediolateral coordinates of the injection of S1 in the opposite hemisphere. Sparse connections were also observed with PV. Note that since ipsilateral label in S1 and 3a from this injection was undercounted (see Connections of S1, above), percentages of label for other fields, including callosal label described here, are overstated as shown in Figure 9A and C. Moreover, we did not attempt to limit our injections to myelin-dense or myelin-light portions of S1; thus, ipsilateral and contralateral connections shown are for both zones.

Callosal connections of area 3a varied between the 2 cases (Fig. 8A,B). In both cases, the densest callosal label was in contralateral area 3a. In one case, label was restricted to a homotopic location (Fig. 8A), and in the other case, with much more callosal transport overall, it was scattered across the mediolateral extent of area 3a (Fig. 8B). Labeled cells were also observed in M1 and S1. In one case, label was sparse in S1 and M1 (Fig. 8A), and in another case, it was quite dense (Fig. 8B). Finally, one case had a few labeled cells in F, PR, and cortex just lateral to S1. Interestingly, the case with the more widespread projections actually had the smaller of the 2 injection sites.

Contralateral label from injections in M1 was relatively sparse in all cases and observed in a homotopic location in M1 of the opposite hemisphere (Fig. 8B,C). Three labeled cells were observed in area 3a, and in one case, a few cells were observed in F. In one case (not shown), sparse label was also observed in PP and PV. Finally, callosal projections to F were primarily from a homotopic location in F. Sparse-to-moderate label was observed in M1 and for area 3a for one injection (not shown). Thus, the callosal connections of field F were highly

restricted. On average across cases, callosal label from M1 injections was found primarily in contralateral M1, F, and 3a (Fig. 9). Contralateral label from injections in F was found primarily in F with most of the remainder in M1.

When all cases for all areas are considered together, a common pattern of interhemispheric connections emerges (Fig. 9C). Most callosal connections were to homotopic locations in the opposite hemisphere, with moderate connections to adjacent cortical areas. Thus, callosal connections were less broadly distributed compared with ipsilateral connections.

Discussion

There were several important findings in the present investigation. First, there are 3 well-defined interconnected cortical areas rostral to S1 in the California ground squirrels: area 3a, the primary motor area, and a frontal area, F. Second, ICMS demonstrates a rough topography of M1, but the map was fractured. Third, detailed motor maps revealed a rostral forelimb area and an eye movement region at the rostromedial border for motor cortex. Fourth, cortical architecture, connections, and functional organization of areas 3a and M1 support the hypothesis that they are distinct cortical areas. Fifth, the connections of area 3a in squirrels have similarities with connections of the dysgranular zone (DZ) in rodents and with area 3a in primates suggesting that these regions are homologous in all species.

The Primary Somatosensory Area, S1

There is a wealth of data on the organization and connectivity of S1 in rodents such as rats (e.g., Chapin et al. 1987; Koralek et al. 1990; Hoffer et al. 2003), squirrels (e.g., Sur et al. 1978; Krubitzer et al. 1986), naked mole rats (Henry and Catania 2006), and voles (Campi et al. 2007, 2010) and grasshopper mice (Sarko et al. 2011). In all rodents, S1 is somatotopically organized from hind paw (medial) to face (lateral), but different species have exaggerated representations of different body parts depending on use and innervation density (see Krubitzer and Disbrow 2008; Qi et al. 2008 for review).

It is important to note that the submodality of neural responses within the classically defined S1 region is not homogeneous. This is best exemplified in the study in rats by Chapin and Lin (1984), in which they demonstrate that neurons in granular cortex are responsive to cutaneous stimulation, neurons in perigranular cortex are responsive to joint and cutaneous stimulation, and neurons in dysgranular cortex are responsive mostly to stimulation of the joints but can respond to cutaneous stimulation, especially at the borders with granular cortex. They also describe a thin TZ just rostral to granular S1 that appears to contain neurons responsive predominantly to stimulation of the joints. In rodents other than rats and mice, such as squirrels, S1 is also architectonically heterogeneous with a large unmyelinated/unresponsive zone (UZ; unresponsive to light cutaneous stimuli in an anesthetized animal) separating the densely myelinated face and hand representations. Other species of rodents also exhibit architectonic heterogeneities in S1 revealed with myelin and cytochrome oxidase (CO) stains (Catania and Henry 2006; Sarko et al. 2011). In these species, myelin- and CO-dense regions are related to major body part representations, which are separated by myelin-/CO-light regions. Thus, in all rodents

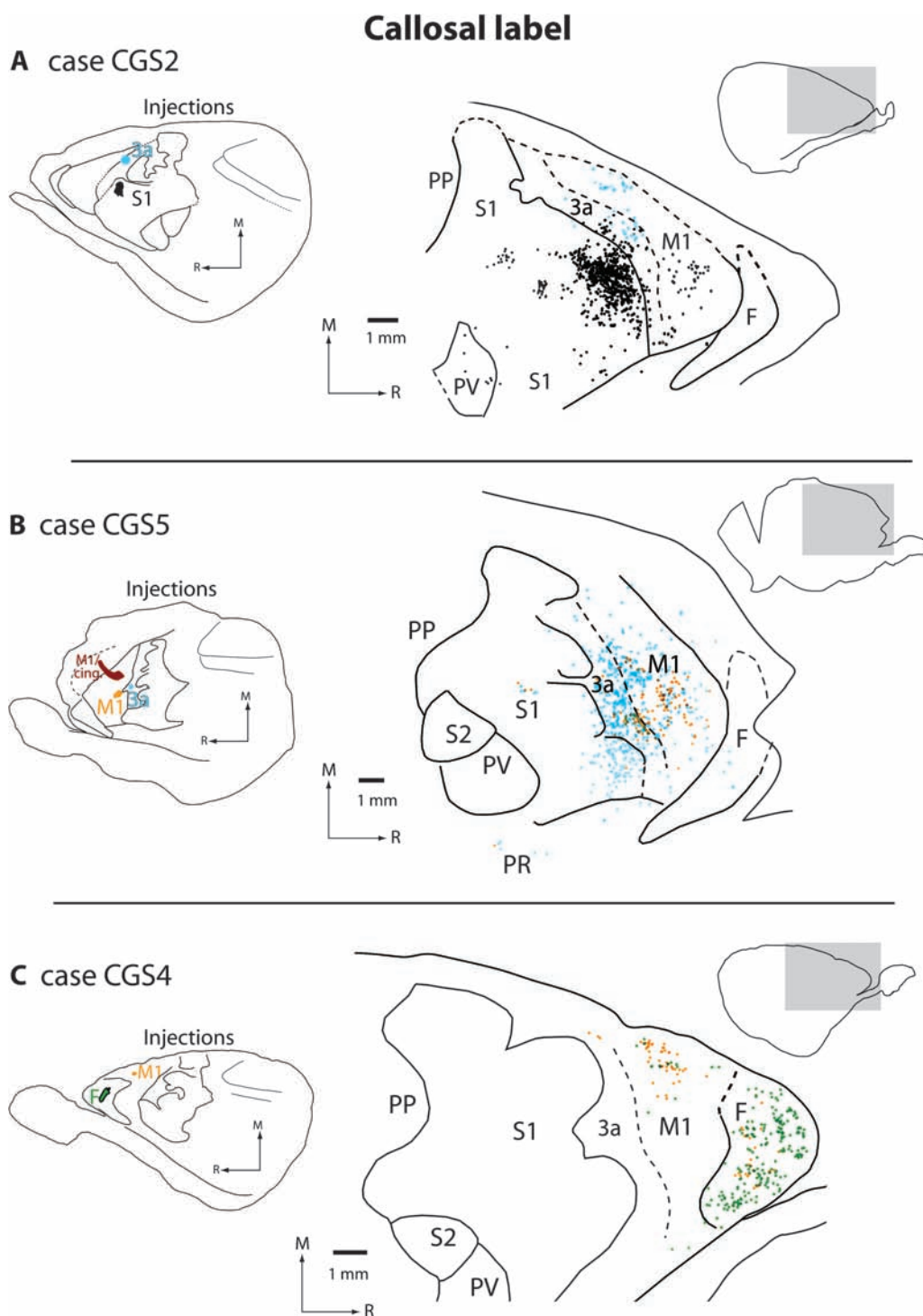


Figure 8. Callosal connections of areas S1, 3a, M1, and F in 3 California ground squirrels. In each panel, the injection locations are depicted at left, the labeled cells in the opposite hemisphere are depicted in the middle, and the location of cells within the opposite hemisphere is depicted as the gray rectangle in the outline of cortex at top right. Callosal connections of S1 (**A**; CGS2) are predominantly in a homotopic location in S1 of the opposite hemisphere. Label was also observed in areas 3a, M1, and PV. Callosal connections of 3a (**A** and **B**) are dense and in one case (**B**; CGS5) are spread throughout 3a. Callosal connections are also observed with M1 and in one case (**B**) with lateral portions of S1 of the opposite hemisphere. In this same case, there are sparse connections with F and PR. Compared with areas S1 and 3a, callosal connections of M1 are sparse (**B** and **C**) and are found predominantly in homotopic locations of M1. There are also sparse connections with 3a and F. Callosal connections of F are predominantly with F of the opposite hemisphere (**C**; CGS4), and there are sparse connections with M1. Conventions as in Figure 6. See Table 1 for abbreviations.

examined, S1 is heterogeneous in appearance, but the geometric relationship of granular/myelin-/CO-dense body part representations to dysgranular/myelin-/CO-light regions is different in different rodents.

Cortical connections of S1 in rodents are most dense with S2, PV, cortex immediately caudal to S1 and motor cortex (Akers and Killackey 1978; Jones et al. 1978; Krubitzer et al. 1986; Koralek et al. 1990; Fabri and Burton 1991a), although

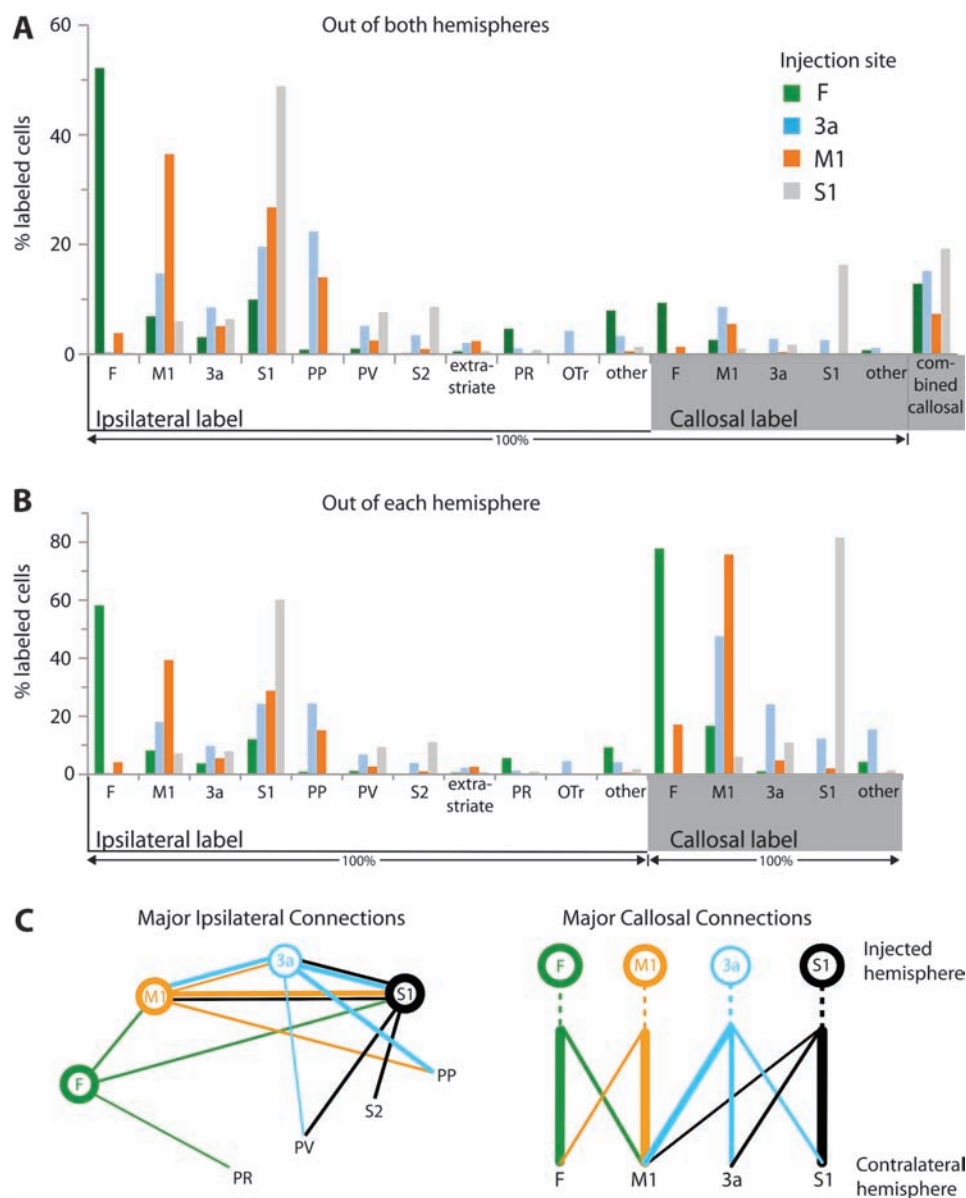


Figure 9. Average proportion of labeled cells observed in different areas of the neocortex following injections in areas F, 3a, M1, and S1. Proportions were calculated in 2 ways: as the number of cells observed in a particular cortical field as a fraction of total cells found in both hemispheres (A) and in each hemisphere separately (B). For each field injected, proportions were averaged across all cases with injections in that field. Data from callosally transported label in the contralateral hemisphere are at right denoted by the gray box in (A) and (B). "Combined callosal label" at far right in (A) is the sum of label in the next 5 groups of bars to the left. (C) depicts a schematic of ipsilateral and callosal connections of F, M1, 3a, and S1. The thicknesses of lines represent mean normalized connection strengths across cases. Line thickness \propto mean $([\text{labeled cells in a field}/\text{total labeled cells in hemisphere}]^{1/2})$. Connections that account for less than 5% of labeled cells are not depicted. Connectivity is complex and the injection sites share many of the same inputs. Relative connection strengths, however, vary between different areas.

several of these studies included injection sites in both granular and dysgranular (unmyelinated) portions of S1 (Akers and Killackey 1978; Krubitzer et al. 1986; Fabri et al. 1990). Studies that specifically examine the connections of granular versus dysgranular (barrel septa) cortex in rats, however, demonstrate differential connectivity within S1 (e.g., Chapin and Lin 1984; see below for further discussion; Kim and Ebner 1999; Lee et al. 2011). Specifically, the latter investigations demonstrate that the nongranular septal cortex has extrinsic connections with PPC. Koralek et al. (1990) attempted a similar study in rats but used an architectonic template so that all connection results were warped onto a single architectonic background (e.g., see their Figs 6 and 7) making it difficult to interpret their results.

Findings of differential connectivity within S1, neural response properties and architecture raise the issue of whether such dysgranular regions should be considered part of S1 or part of a separate completely embedded field (see Discussion below).

Area 3a

Although area 3a has not been definitively identified in rats or mice, the idea that the rostral TZ in rats is homologous to area 3a in nonrodent mammals has been previously discussed by Chapin and Lin (1984), although they do not include DZ as part of area 3a but as a subdivision of S1. A recent architectonic study in which the tree squirrel brain was cut in a standard plane of section and stained for Nissl indicates that like DZ and TZ in rats,

area 3a in squirrels has a reduced granular layer and larger pyramidal cells in layer 5 compared with granular cortex (Wong and Kaas 2008). Area 3a in nonrodent mammals has a similar cytoarchitecture. Moreover, in our earlier electrophysiological study of this region in ground squirrels (Slutsky et al. 2000), we found a complete representation of deep receptors of the muscles and joints and noted similarities in appearance, location, and neural response properties between this rostral area in squirrels, the TZ + DZ of rats, and area 3a of nonrodent mammals. We suggested that all of these areas are homologous. Here, we demonstrate that microstimulation of neurons in cortex rostral to S1, the same region containing neurons responsive to stimulation of deep but not cutaneous receptors, often evokes movements of the contralateral body, and that the connections of area 3a are distinct from those of S1 (see Fig. 9). Although there are similarities in cortical connections between M1 and 3a, they are not identical, and thalamocortical connections of these 2 fields are distinct (Cooke et al. 2007). These properties provide additional support for the earlier contention that this field is a homologue to area 3a defined in mammals such as ferrets (Leclerc et al. 1993; Rice et al. 1993), raccoons (“kinesthetic cortex,” Johnson et al. 1982; Feldman and Johnson 1988), and primates (e.g., Powell and Mountcastle 1959; Stepniewska et al. 1993; Huffman and Krubitzer 2001a; Krubitzer et al. 2004; Wang et al. 2007; see Fig. 10). This comparison is particularly compelling when the ipsilateral cortical connections of 3a in squirrels are compared with those in primates such as the marmoset (Huffman and Krubitzer 2001a) and the tree shrew (Remple et al. 2007). In all 3 species, connections of area 3a are sparse with the myelin-dense portions of S1 and particularly dense with cortex immediately caudal to S1. The region caudal to S1 has been termed parietal medial (PM/PP) in squirrels, the PPC in rats and tree shrews, and area 1/2 or PP in marmosets. Area 3a in squirrels also receives input from S2, PV, motor cortex, and extrastriate visual cortex caudal to PP. In monkeys and tree shrews, 3a has similar connections with these fields, with additional connections to supplementary motor area (SMA), premotor cortex, and additional regions of PPC (e.g., Guldin et al. 1992; Darian-Smith et al. 1993; Huffman and Krubitzer 2001a; Remple et al. 2007; see Krubitzer and Disbrow 2008 for review).

What parts of cortex in squirrels and rats might be homologous to nonrodent 3a? In the squirrel, we propose that area 3a includes not only a strip of cortex between S1 and M1 but also the unmyelinated zone that separates the face and forepaw representations in S1 corresponding to the UZ of Sur et al. (1978). Chapin and Lin (1984) found rat DZ (which they compared with squirrel UZ) to be unresponsive under anesthesia and responsive to muscle and joint stimulation in awake or lightly anesthetized preparations. We suggest that these portions of squirrel cortex are homologous with the DZ (and perigranular) + TZ in rats. This is based on 4 important observations. First, all of these regions are rich in callosal connections in both rats (e.g., Akers and Killackey 1978; Koralek et al. 1990) and squirrels (Gould and Kaas 1981). Second, both are distinguished by distinct thalamic input. Granular/myelinated cortex has dense input from the ventral posterior nucleus, while dysgranular/unmyelinated zones receive dense inputs from the medial division of the posterior nucleus in both rats (Killackey 1973; Killackey and Leshin 1975; Koralek et al. 1988; Lu and Lin 1993) and squirrels (Gould et al. 1989; Cooke et al. 2007). Third, the present study

indicates that in squirrels, area 3a has connections that are distinct from the highly myelinated S1 and has dense connections with PPC. In rats, studies of extrinsic cortico-cortical connections of granular and dysgranular (and perigranular) cortex, in which injection sites were clearly limited to the granular versus nongranular zones demonstrate that dysgranular cortex projects to PPC, among other regions (Kim and Ebner 1999; Lee et al. 2011). The correspondence between rat barrel septa and squirrel 3a cannot be entirely equivalent since barrels/septa represent an extremely derived system and may only be one specialized part of the whole rat DZ body representation. Finally, the present and previous studies in anesthetized squirrels (Sur et al. 1978; Slutsky et al. 2000) and studies in anesthetized and awake rats (Chapin and Lin 1984) demonstrate different functional properties in granular (darkly myelinated S1) versus DZ + TZ (3a). The former contains neurons predominantly responsive to cutaneous receptors, and the latter contains neurons responsive to joint and/or cutaneous stimulation (although under anesthesia, neurons in DZ are unresponsive to both types of stimulation). Our proposition for homology rests on the supposition that most or all of nongranular cortex in S1, sometimes proposed as separate regions, is really a single field (e.g., DZ, TZ, and perhaps the septal space surrounding barrels), and previous investigators also conclude that this is the case (e.g., Fabri and Burton 1991b; see Alloway 2008 for review).

Because area 3a in squirrels shares a number of features with the DZ/TZ in rats and area 3a in other mammalian orders, we consider this field homologous and thus suggest that it was present in the common ancestor of primates, carnivores, and rodents (Fig. 10). The degree to which portions of this field extend into granular S1 is different in different species, with a complete segregation in primates, a partial segregation in squirrels, and complete interdigitation in murine rodents. An alternate but less likely scenario is that a 3a-like field has evolved independently multiple times.

The present results indicate that squirrel area 3a is involved in motor processing in agreement with other studies in rodents. Alloway (2008) proposes a sensory role for rat granular barrels and motor control function for septa. Further evidence for a motor role for part of a traditionally “sensory” field comes from a recent study in mice, in which whisker movements could be evoked by electrical stimulation in S1 (Matyas et al. 2010). Chemical inactivation of S1 prevented the mouse from making normal sensory-evoked whisker retractions, while inactivation of a whisker retraction site in M1 had no effect on this behavior. In the mouse, therefore, M1 control of whisker retraction appears to occur via S1, while protraction occurs more directly from M1 to subcortical structures. Thus, distinct motor functions were associated with S1 and M1, although it is unknown if all of S1 subserves a distinct function or if only portions of S1 such as septal/DZ are involved.

The Frontal Area, F

The field we call F has been previously described in the tree squirrel (Wong and Kaas 2008). Area F is myeloarchitectonically distinct from M1, and connective patterns, including projections from M1, somatosensory areas, PP, and the mediodorsal nucleus of the thalamus (Cooke et al. 2007) suggest involvement in sensorimotor processing. It is clear that area F is not the frontal eye field (FEF). No movements were

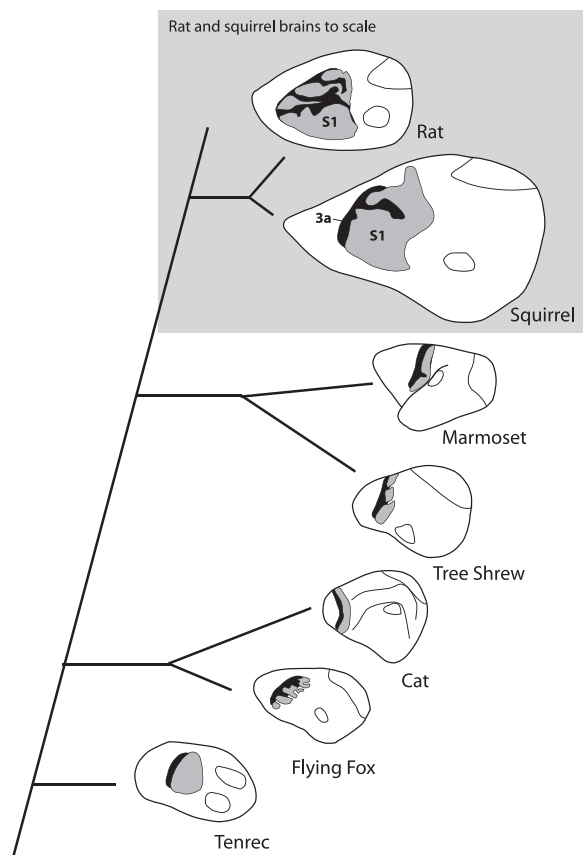


Figure 10. Evolutionary relationship of some mammals with an identified (or in the case of the rat, proposed) area 3a. Branch lengths of cladogram are not to scale. Each species is represented by a lateral view of a schematic brain showing 3a (black) and S1 (gray) as well as primary auditory and visual fields (adapted from: cat—Felleman et al. 1983; rat—Chapin and Lin 1984; tenrec—Krubitzer et al. 1997; flying fox—Krubitzer et al. 1998; marmoset—Huffman and Krubitzer 2001a; tree shrew—Wong and Kaas 2009). All brains except rat and squirrel are not to scale. Area 3a is widespread in the mammalian lineage; this fact and shared properties suggest that rat dysgranular cortex is homologous with 3a in squirrels in other mammals.

evoked by stimulation in F, while some eye movements were evoked in moderately myelinated, rostral-medial M1. Nor does area F seem to correspond to rat AGm or “medial prefrontal cortex” (Ongur and Price 2000), which contains a rodent eye field (e.g., Leonard 1969). Further, most of AGm is far medial and wraps onto the medial wall. While the location and some of the connections of area F indicate that it may correspond to a subdivision of prefrontal cortex or premotor cortex, further exploration of area F is needed to resolve this issue.

The Primary Motor Area, M1

As noted in the Introduction, previous studies of the functional organization of motor cortex (M1) were limited to rats (Hall and Lindholm 1974; Donoghue and Wise 1982; Donoghue and Parham 1983; Gioanni and Lamarche 1985; Neafsey et al. 1986; Kleim et al. 1998; Brecht et al. 2004; Haiss and Schwarz 2005; Ramanathan et al. 2006; Tandon et al. 2008) and mice (Li and Waters 1991; Pronichev and Lenkov 1998; Tennant et al. 2011) (Fig. 11A–F). In these studies, ICMS produced topographically organized maps of the body with the hindlimb represented medially, followed by the forelimb laterally. In some studies, portions of the face were represented lateral to the forelimb, and in all studies, the vibrissae were represented rostrally. In

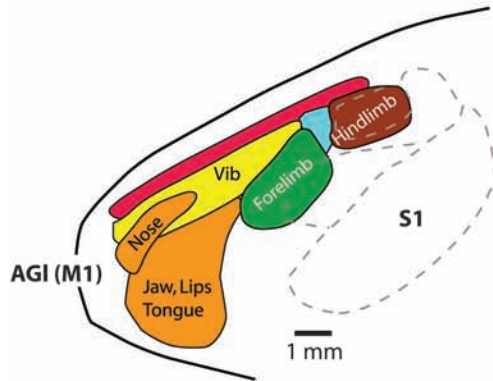
many of these studies, an additional forelimb representation was observed rostrally and termed the rostral forelimb area (RFA; e.g., Neafsey and Sievert 1982).

In rats and mice, this low-threshold excitable cortex (M1) is cytoarchitecturally identified as agranular cortex, with a very thin or nonexistent layer IV (e.g., Donoghue and Wise 1982; Tennant et al. 2011). Agranular cortex is divided into lateral (AGl) and medial (AGm) regions, based on differences in layers II, III, and V (Donoghue and Wise 1982; Brecht et al. 2004). Studies examining the correspondence between functional maps and these architectonic fields have produced conflicting results. Donoghue and Wise (1982) reported a complete representation of body movements in AGl, including vibrissae, but could not evoke any low-threshold (<65 μ A) movements from sites in AGm. They therefore described AGl as coinciding with M1, while they compared AGm with the primate SMA or M2 based on connections and higher ICMS thresholds. In contrast, Neafsey et al. (1986) did report ICMS movements in AGm, observing that a majority of vibrissae movements along with eye and head movements were found there. They compared AGm with primate FEF, describing it as serving “attentional/orientation functions.” (They also described the distinct rostral representations of the fore- and hindlimb as possibly corresponding to SMA.) A more recent study (Brecht et al. 2004) agreed with Neafsey et al. (1986) on the role of AGm as representing vibrissae, and further described it as having stimulation thresholds similar to AGl, but being much more sensitive to anesthetic level (perhaps explaining differences with past results). Brecht et al. (2004) differ, however, in their inclusion of AGl and AGm (and cingulate area 1) in M1.

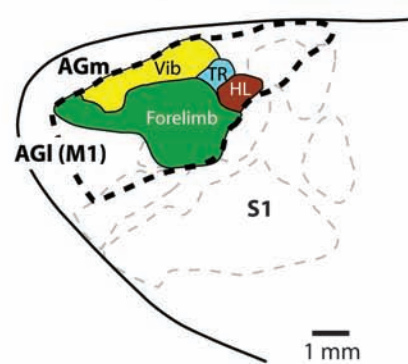
When comparing our results in squirrels with those observed in previous studies in rats and mice, it is important to remember that microstimulation results may be significantly altered by anesthetic type and level (e.g., Tandon et al. 2008), stimulation parameters (e.g., Hall and Lindholm 1974; Krubitzer et al. 2011 for review), and the use of ascending versus descending threshold determination. Despite these potential complications, we found that as in rats and mice, ICMS over a large region of squirrel frontal cortex evoked motor movements at low current thresholds. We observed a gross somatotopic organization of body movements, with a rough medial-lateral progression of hindlimb, trunk, forelimb, and face movement representations (Figs 4 and 5). While we did observe what appeared to be a rostral forelimb representation, we did not observe a distinct medial vibrissae representation in squirrels. We did, however, observe a small eye movement region at the medial border of our excitable region surrounded by vibrissae sites as well as the ear representation, which may be involved in orientation. Compared with studies in rats, our motor maps in squirrels were fractured in that multiple body part movement representations were observed at different locations. This distinction may not be a true difference, but an artifact of differences in map construction and current levels used. Composite maps made from data from several animals can obscure fractured organization, but when densely sampled motor maps of individual animals are examined, as in mice, fractured maps are observed (Tennant et al. 2011). Further, different currents used to determine threshold of movement may also affect the size of the movement field as well as the size of the body part representations within the map and thus map configurations across studies.

The Organization of Motor Cortex in Rodents

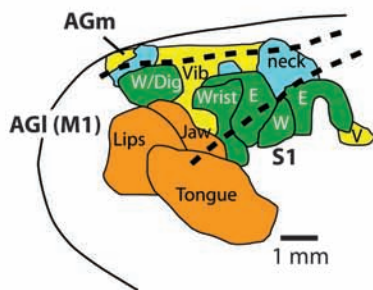
A Rat: Hall and Lindholm, 1974



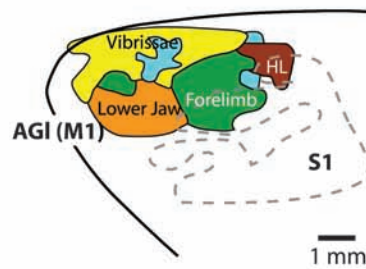
B Rat: Donoghue and Wise, 1982



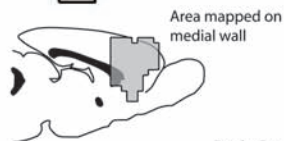
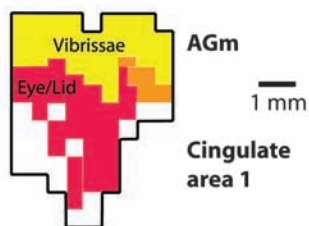
C Rat: Neafsey et al., 1986



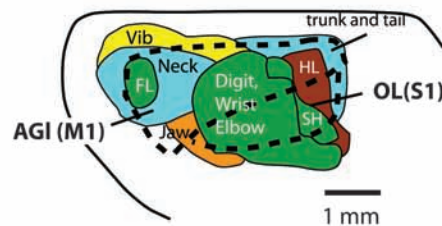
D Rat: Tandon et al., 2008



E Rat: Brecht et al., 2004



F Mouse: Tennant et al., 2010



G Tree squirrel: This study

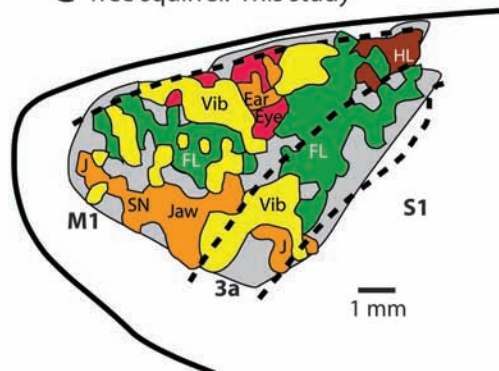


Figure 11. Topographic organization of M1 (AGI) as described in different studies in rats (A–E), mice (F), and squirrels (G). Despite the differences in stimulation parameters and anesthetic, the maps in rats generated in different laboratories are remarkably similar. Some of these drawings were generated by combining multiple maps from a single publication (e.g., C). Some drawings are from maps chosen from one of several that were generated based on a particular current threshold (D). The squirrel motor map (based on case TS1 in Fig. 4) appears fractured compared with other maps, but the general organization is similar. Note that a second representation of the forelimb located rostrally is observed in some studies in rats (C and D), mice (F), and squirrels (G). Body part representations have been color coded. All drawings are to scale except the mouse, which is presented at twice the scale of other maps. Data are redrawn from previous studies noted. All architectonic boundaries illustrated in previous studies are drawn here as dashed lines. See Table 1 for abbreviations. Conventions as in previous figures.

We also observed that cortex immediately caudal to M1 contained a low-threshold motor map that overlaps with a somatosensory representation of receptors of joints and muscles of the contralateral body (Slutsky et al. 2000). This field, area 3a, is both architectonically and functionally distinct from M1. As noted in the previous section, a sensorimotor overlap has been observed in rats, but in rats, this overlap is with cutaneous S1 and not an intervening field (see above for further discussion).

Taken together, these functional data suggest that the large low-threshold zone in squirrels may be composed of 2 fields: a caudal field overlapping with the moderately myelinated area 3a and a rostromedial field (M1) that also contains a complete representation of the body including a medially located eye movement field. If our interpretation of the granular and dysgranular regions of rat S1 discussed above is correct, then rat TZ/DZ is homologous with 3a, and rat AGI alone is homologous with M1 in other mammals. An alternate hypothesis is that in murine rodents, overlap of S1/DZ/M1 represents a derivation of the eutherian ancestral motor cortex specific to the behavior of these animals.

As noted above, the internal organization we observed in squirrel M1 was fractured, suggesting that organizational principles other than somatotopy may contribute to the final pattern of the motor map (Aflalo and Graziano 2006). Aside from somatotopy, another organizing principle may be representations of functionally related body parts that are used in combination during common natural movements. Although limited on this point, our results point to an anatomical substrate for this feature of map organization in that a given motor representation in M1 (e.g., forepaw/forelimb) receives input from similar body part representations such as the wrist and forelimb and from nonadjacent body part representations such as from the vibrissae, hindlimb, and upper lip (e.g., Figs 6B and 7B). Such connections and movement representations are both likely to reflect the behaviors and sensorimotor specializations of each species. For example, early studies of extrinsic cortical connections of M1 in mice (e.g., Porter and White 1983) demonstrated that the vibrissae representation had strong projections to a homotopic location in S1, contralateral M1, and ipsilateral and contralateral S2. In rats, projections to AGI are from S1, S2, and AGm. The S1 projections are mainly from dysgranular cortex (Donoghue and Parham 1983). Recent studies in rats demonstrate differential projections of the whisker and forepaw representations (Alloway et al. 2009; Colechio and Alloway 2009) with strong callosal connections between whisker representations and less dense callosal projections from the forepaw representation. Overall ipsilateral patterns of connectivity of M1 in rats (Colechio and Alloway 2009) were very similar to those that we observed in squirrels with one difference. In rats, the whisker representation in M1 (AGI) had dense projections to PPC and the forelimb had sparse connections to PP, whereas in squirrels, the pattern appeared to be reversed.

Such differential connectivity between M1 and PPC may be linked to behavioral specialization. In rats, whisking behavior plays a central role in navigation and exploration (Vincent 1912), and it is likely that in generating an internal coordinate system for the guidance of these behaviors, whisking plays a larger role in rats than squirrels. Although squirrels possess whiskers, whisking is less important in navigation and exploration, and vision plays a much larger role in these behaviors. Furthermore, squirrels are highly dexterous and use their paws (and eyes) extensively for object exploration. Thus,

the way an animal updates the internal representation of its location and surrounding objects likely relies on different sensory and motor inputs to PPC in these species. In primates, PPC is dominated by visual inputs as well as proprioceptive inputs from the hand and shoulder (Huffman and Krubitzer 2001b; Padberg et al. 2005; Stepniewska et al. 2009). Not surprisingly, connections of some posterior parietal areas in primates are predominantly with representations of the forelimb in M1, 3a, and other motor areas (e.g., Cavada and Goldman-Rakic 1989a, 1989b; Huffman and Krubitzer 2001b; Stepniewska et al. 2009). Like primates, squirrels' motor connectivity reflects a more forelimb-centered lifestyle than that of rats.

Taken together, studies in squirrels and other rodents demonstrate that there are features of squirrel motor cortex organization that are similar to the murine rodents that have been studied including the presence of a well-defined M1, a TZ (area 3a) between S1 and M1, and a rostral forelimb representation. From an evolutionary perspective, the data on the few species examined indicate that the ancestor of all rodents possessed these features of organization, and they may be common to mammals in general. On the other hand, some aspects of organization appear to be unique to squirrels including strong connections between 3a and PPC and divisions of extrastriate visual cortex and differential connections of vibrissae and forelimb representations in M1. These types of connections have been observed in other highly visual mammals such as primates and tree shrews. While squirrels are phylogenetically distinct from primates and tree shrews, it is possible that the independent expansion of visual cortex and visuomotor adaptations in these lineages led to the independent evolution of similar properties and connections of sensorimotor, visual, and posterior parietal cortex.

Funding

This work was supported in part by a McDonnell Foundation grant; National Institutes of Health awards (R01-NS035103, IOS-0743924 to L.K., NS59262 to D.C.).

Notes

We thank Katy Campi and Adele Seelke for help with this manuscript. *Conflict of Interest*: None declared.

References

- Aflalo TN, Graziano MS. 2006. Possible origins of the complex topographic organization of motor cortex: reduction of a multidimensional space onto a two-dimensional array. *J Neurosci*. 26:6288–6297.
- Akers RM, Killackey HP. 1978. Organization of corticocortical connections in the parietal cortex of the rat. *J Comp Neurol*. 181:513–538.
- Alloway KD. 2008. Information processing streams in rodent barrel cortex: the differential functions of barrel and septal circuits. *Cereb Cortex*. 18:979–989.
- Alloway KD, Smith JB, Beauchemin KJ, Olson ML. 2009. Bilateral projections from rat M1 whisker cortex to the neostriatum, thalamus, and claustrum: forebrain circuits for modulating whisking behavior. *J Comp Neurol*. 515:548–564.
- Brecht M, Krauss A, Muhammad S, Sinai-Esfahani L, Bellanca S, Margrie TW. 2004. Organization of rat vibrissa motor cortex and adjacent areas according to cytoarchitectonics, microstimulation, and intracellular stimulation of identified cells. *J Comp Neurol*. 479:360–373.
- Campi KL, Bales KL, Grunewald R, Krubitzer L. 2010. Connections of auditory and visual cortex in the prairie vole (*Microtus ochrogaster*): evidence for multisensory processing in primary sensory areas. *Cereb Cortex*. 20:89–108.

- Campi KL, Collins CE, Todd WD, Kaas J, Krubitzer L. 2011. Comparison of area 17 cellular composition in laboratory and wild-caught rats including diurnal and nocturnal species. *Brain Behav Evol.* 77:116-130.
- Campi KL, Karlen SJ, Bales KL, Krubitzer L. 2007. Organization of sensory neocortex in prairie voles (*Microtus ochrogaster*). *J Comp Neurol.* 502:414-426.
- Campi KL, Krubitzer L. 2010. Comparative studies of diurnal and nocturnal rodents: differences in lifestyle result in alterations in cortical field size and number. *J Comp Neurol.* 518:4491-4512.
- Catania KC, Henry EC. 2006. Touching on somatosensory specializations in mammals. *Curr Opin Neurobiol.* 16:467-473.
- Cavada C, Goldman-Rakic PS. 1989a. Posterior parietal cortex in rhesus monkey: I. Parcellation of areas based on distinctive limbic and sensory corticocortical connections. *J Comp Neurol.* 287:393-421.
- Cavada C, Goldman-Rakic PS. 1989b. Posterior parietal cortex in rhesus monkey: II. Evidence for segregated corticocortical networks linking sensory and limbic areas with the frontal lobe. *J Comp Neurol.* 287:422-445.
- Chapin JK, Lin C-L. 1984. Mapping the body representation in the SI cortex of anesthetized and awake rats. *J Comp Neurol.* 229:199-213.
- Chapin JK, Sadeq M, Guise JLU. 1987. Corticocortical connections within the primary somatosensory cortex of the rat. *J Comp Neurol.* 263:326-346.
- Colechio EM, Alloway KD. 2009. Differential topography of the bilateral cortical projections to the whisker and forepaw regions in rat motor cortex. *Brain Struct Funct.* 213:423-439.
- Cooke DF, Padberg J, Zahner T, Grunewald B, Krubitzer L. Complex movements evoked by microstimulation of motor cortex in the California ground squirrel (*Spermophilus beecheyi*). Program No. 277.18. 2008 Neuroscience Meeting Planner. Washington, DC: Society for Neuroscience, 2008. Online. [abstract].
- Cooke DF, Padberg J, Zahner T, Krubitzer L. Thalamocortical connections of motor and sensorimotor cortical fields in California ground squirrel (*Spermophilus beecheyi*). Program No. 193.18. 2007 Neuroscience Meeting Planner. San Diego, CA: Society for Neuroscience, 2007. Online. [abstract].
- Darian-Smith C, Darian-Smith I, Burman K, Ratcliffe N. 1993. Ipsilateral cortical projections to areas 3a, 3b, and 4 in the macaque monkey. *J Comp Neurol.* 335:200-213.
- Donoghue JP, Parham C. 1983. Afferent connections of the lateral agranular field of the rat motor cortex. *J Comp Neurol.* 217:390-404.
- Donoghue JP, Wise SP. 1982. The motor cortex of the rat: cytoarchitecture and microstimulation mapping. *J Comp Neurol.* 212:76-88.
- Fabri M, Alloway K, Burton H. 1990. Multiple ipsilateral connections of SI in rats. *Soc Neurosci Abs.* 16:228.
- Fabri M, Burton H. 1991a. Ipsilateral cortical connections of primary somatic sensory cortex in rats. *J Comp Neurol.* 311:405-424.
- Fabri M, Burton H. 1991b. Topography of connections between primary somatosensory cortex and posterior complex in rat: a multiple fluorescent tracer study. *Brain Res.* 538:351-357.
- Fang PC, Stepniowska I, Kaas JH. 2005. Ipsilateral cortical connections of motor, premotor, frontal eye, and posterior parietal fields in a prosimian primate, *Otolemur garnetti*. *J Comp Neurol.* 490:305-333.
- Feldman SH, Johnson JI. 1988. Kinesthetic cortical area anterior to primary somatic sensory cortex in the raccoon (*Procyon lotor*). *J Comp Neurol.* 277:80-95.
- Felleman DJ, Wall JT, Cusick CG, Kaas JH. 1983. The representation of the body surface in S-I of cats. *J Neurosci.* 3:1648-1669.
- Gallyas F. 1979. Silver staining of myelin by means of physical development. *Neurology.* 1:203-209.
- Gioanni Y, Lamarche M. 1985. A reappraisal of rat motor cortex organization by intracortical microstimulation. *Brain Res.* 344:49-61.
- Gould HJ 3rd, Whitworth RH Jr, LeDoux MS. 1989. Thalamic and extrathalamic connections of the dysgranular unresponsive zone in the grey squirrel (*Sciurus carolinensis*). *J Comp Neurol.* 287:38-63.
- Gould HJI, Cusick CG, Pons TP, Kaas JH. 1986. The relationship of corpus callosum connections to electrical stimulation maps of motor, supplementary motor, and the frontal eye fields in owl monkeys. *J Comp Neurol.* 247:297-325.
- Gould HJI, Kaas JH. 1981. The distribution of commissural terminations in somatosensory areas I and II of the grey squirrel. *J Comp Neurol.* 196:489-504.
- Graziano MS, Taylor CS, Moore T, Cooke DF. 2002. The cortical control of movement revisited. *Neuron.* 36:349-362.
- Guldin WO, Akbarian S, Grusser OJ. 1992. Cortico-cortical connections and cytoarchitectonics of the primate vestibular cortex: a study in squirrel monkeys (*Saimiri sciureus*). *J Comp Neurol.* 326:375-401.
- Haiss F, Schwarz C. 2005. Spatial segregation of different modes of movement control in the whisker representation of rat primary motor cortex. *J Neurosci.* 25:1579-1587.
- Hall RD, Lindholm EP. 1974. Organization of motor and somatosensory neocortex in the albino rat. *Brain Res.* 66:23-38.
- Hall WC, Kaas JH, Killackey H, Diamond IT. 1971. Cortical visual areas in grey squirrel (*Sciurus carolinensis*): a correlation between cortical evoked potential maps and architectonic subdivisions. *J Neurophysiol.* 34:437-452.
- Henry EC, Catania KC. 2006. Cortical, callosal, and thalamic connections from primary somatosensory cortex in the naked mole-rat (*Heterocephalus glaber*), with special emphasis on the connectivity of the incisor representation. *Anat Rec A Discov Mol Cell Evol Biol.* 288:626-645.
- Hoffer ZS, Hoover JE, Alloway KD. 2003. Sensorimotor corticocortical projections from rat barrel cortex have an anisotropic organization that facilitates integration of inputs from whiskers in the same row. *J Comp Neurol.* 466:525-544.
- Huchon D, Chevret P, Jordan U, Kilpatrick CW, Ranwez V, Jenkins PD, Brosius J, Schmitz J. 2007. Multiple molecular evidences for a living mammalian fossil. *Proc Natl Acad Sci U S A.* 104:7495-7499.
- Huchon D, Madsen O, Sibbald MJ, Ament K, Stanhope MJ, Catzeflis F, de Jong WW, Douzery EJ. 2002. Rodent phylogeny and a timescale for the evolution of Glires: evidence from an extensive taxon sampling using three nuclear genes. *Mol Biol Evol.* 19:1053-1065.
- Huffman KJ, Krubitzer LA. 2001a. Area 3a: topographic organization and connections in marmoset monkeys. *Cereb Cortex.* 11:849-867.
- Huffman KJ, Krubitzer LA. 2001b. Thalamo-cortical connections of areas 3a and M1 in marmoset monkeys. *J Comp Neurol.* 435:291-310.
- Johnson JI, Ostapoff E-M, Warach S. 1982. The anterior border zones of primary somatic sensory (SI) neocortex and their relation to cerebral convolutions, shown by micromapping of peripheral projections to the region of the fourth forepaw digit representation in raccoons. *Neuroscience.* 7:915-936.
- Jones EG, Coulter JD, Hendry SHC. 1978. Intracortical connectivity of architectonic fields in the somatic sensory, motor and parietal cortex of monkeys. *J Comp Neurol.* 181:291-348.
- Kaas JH. 1983. What, if anything, is SI? Organization of first somatosensory area of cortex. *Physiol Rev.* 63:206-230.
- Kaas JH, Hall WD, Diamond IT. 1972. Visual cortex of the grey squirrel (*Sciurus carolinensis*): architectonic subdivisions and connections from the visual thalamus. *J Comp Neurol.* 145:273-306.
- Killackey HP. 1973. Anatomical evidence for cortical subdivisions based on vertically discrete thalamic projections from the ventral posterior nucleus to cortical barrels in the rat. *Brain Res.* 51:326-331.
- Killackey HP, Leshin S. 1975. The organization of specific thalamocortical projections to the posteromedial barrel subfield of the rat somatic sensory cortex. *Brain Res.* 86:469-472.
- Kim U, Ebner FF. 1999. Barrels and septa: separate circuits in rat barrels field cortex. *J Comp Neurol.* 408:489-505.
- Kleim JA, Barbay S, Nudo RJ. 1998. Functional reorganization of the rat motor cortex following motor skill learning. *J Neurophysiol.* 80:3321-3325.
- Koralek KA, Jensen KF, Killackey HP. 1988. Evidence for two complementary patterns of thalamic input to the rat somatosensory cortex. *Brain Res.* 463:346-351.
- Koralek KA, Olavarria J, Killackey HP. 1990. Areal and laminar organization of corticocortical projections in rat somatosensory cortex. *J Comp Neurol.* 299:133-150.
- Krubitzer L, Campi KL, Cooke DF. 2011. All rodents are not the same: a modern synthesis of cortical organization. *Brain Behav Evol.* 2011 Jun 23. [Epub ahead of print].

- Krubitzer L, Clarey J, Tweedale R, Calford M. 1998. Interhemispheric connections of somatosensory cortex in the flying fox. *J Comp Neurol*. 402:538-559.
- Krubitzer L, Disbrow E. 2008. The evolution of parietal areas involved in hand use in primates. In: Gardner E, Kaas JH, editors. *Somatosensation*. London: Elsevier. p. 183-214.
- Krubitzer L, Huffman KJ, Disbrow E, Recanzone G. 2004. Organization of area 3a in macaque monkeys: contributions to the cortical phenotype. *J Comp Neurol*. 471:97-111.
- Krubitzer L, Künzle H, Kaas J. 1997. Organization of sensory cortex in a Madagascan insectivore, the tenrec (*Echinops telfairi*). *J Comp Neurol*. 379:399-414.
- Krubitzer LA, Sesma MA, Kaas JH. 1986. Microelectrode maps, myeloarchitecture, and cortical connections of three somatotopically organized representations of the body surface in the parietal cortex of squirrels. *J Comp Neurol*. 250:403-430.
- Leclerc SS, Rice FL, Dykes RW, Pourmoghadam K, Gomez CM. 1993. Electrophysiological examination of the representation of the face in the suprasylvian gyrus of the ferret: a correlative study with cytoarchitecture. *Somatosens Mot Res*. 10:133-159.
- Lee T, Alloway KD, Kim U. 2011. Interconnected cortical networks between primary somatosensory cortex septal columns and posterior parietal cortex in rat. *J Comp Neurol*. 519:405-419.
- Leonard CM. 1969. The prefrontal cortex of the rat. I. Cortical projection of the mediodorsal nucleus. II. Efferent connections. *Brain Res*. 12:321-343.
- Li CX, Waters RS. 1991. Organization of the mouse motor cortex studied by retrograde tracing and intracortical microstimulation (ICMS) mapping. *Can J Neurol Sci*. 18:28-38.
- Lu SM, Lin RS. 1993. Thalamic afferents of the rat barrel cortex: a light- and electron-microscopic study using Phaseolus vulgaris leucoagglutinin as an anterograde tracer. *Somatosens Mot Res*. 10:1-16.
- Luethke LE, Krubitzer LA, Kaas JH. 1988. Cortical connections of electrophysiologically and architectonically defined subdivisions of auditory cortex in squirrels. *J Comp Neurol*. 268:181-203.
- Manger PR, Cort J, Ebrahim N, Goodman A, Henning J, Karolia M, Rodrigues SL, Strkalj G. 2008. Is 21st century neuroscience too focussed on the rat/mouse model of brain function and dysfunction? *Front Neuroanat*. 2:5.
- Matyas F, Sreenivasan V, Marbach F, Wacongne C, Barsy B, Mateo C, Aronoff R, Petersen CC. 2010. Motor control by sensory cortex. *Science*. 330:1240-1243.
- Merzenich MM, Kaas JH, Roth GL. 1976. Auditory cortex in the grey squirrel: tonotopic organization and architectonic fields. *J Comp Neurol*. 166:387-402.
- Neafsey EJ, Bold EL, Haas G, Hurley-Gius KM, Quirk G, Sievert CF, Terreberry RR. 1986. The organization of the rat motor cortex: a microstimulation mapping study. *Brain Res*. 396:77-96.
- Neafsey EJ, Sievert C. 1982. A second forelimb motor area exists in rat frontal cortex. *Brain Res*. 232:151-156.
- Ongur D, Price JL. 2000. The organization of networks within the orbital and medial prefrontal cortex of rats, monkeys and humans. *Cereb Cortex*. 10:206-219.
- Padberg J, Disbrow E, Krubitzer L. 2005. The organization and connections of anterior and posterior parietal cortex in titi monkeys: do New World monkeys have an area 2? *Cereb Cortex*. 15:1938-1963.
- Porter LL, White EL. 1983. Afferent and efferent pathways of the vibrissal region of primary motor cortex in the mouse. *J Comp Neurol*. 214:279-289.
- Powell TPS, Mountcastle VB. 1959. Some aspects of the functional organization of the cortex of the postcentral gyrus of the monkey: a correlation of findings obtained in a single unit analysis with cytoarchitecture. *Bull Johns Hopkins Hosp*. 105:133-162.
- Pronichev IV, Lenkov DN. 1998. Functional mapping of the motor cortex of the white mouse by a microstimulation method. *Neurosci Behav Physiol*. 28:80-85.
- Qi HX, Preuss TM, Kaas JH. 2008. Somatosensory areas of the cerebral cortex: architectonic characteristics and modular organization. In: Kaas JH, Gardner EP, editors. *The senses: a comprehensive reference*. London: Elsevier. p. 143-169.
- Ramanathan D, Conner JM, Tuszynski MH. 2006. A form of motor cortical plasticity that correlates with recovery of function after brain injury. *Proc Natl Acad Sci U S A*. 103:11370-11375.
- Remple MS, Reed JL, Stepniewska I, Lyon DC, Kaas JH. 2007. The organization of frontoparietal cortex in the tree shrew (*Tupaia belangeri*): II. Connectional evidence for a frontal-posterior parietal network. *J Comp Neurol*. 501:121-149.
- Rice FL, Gomez CM, Leclerc SS, Dykes RW, Moon JS, Pourmoghadam K. 1993. Cytoarchitecture of the ferret suprasylvian gyrus correlated with areas containing multiunit responses elicited by stimulation of the face. *Somatosens Mot Res*. 10:161-188.
- Sarko DK, Leitch DB, Girard I, Sikes RS, Catania KC. 2011. Organization of somatosensory cortex in the Northern grasshopper mouse (*Onychomys leucogaster*), a predatory rodent. *J Comp Neurol*. 519:64-74.
- Sereno MI, Rodman HR, Karten HJ. 1991. Organization of visual cortex in the California ground squirrel. *Soc Neurosci Abs*. 17:844.
- Slutsky DA, Manger PR, Krubitzer L. 2000. Multiple somatosensory areas in the anterior parietal cortex of the California ground squirrel (*Spermophilus beecheyi*). *J Comp Neurol*. 416:521-539.
- Stepniewska I, Cerkevich CM, Fang PC, Kaas JH. 2009. Organization of the posterior parietal cortex in galagos: II. Ipsilateral cortical connections of physiologically identified zones within anterior sensorimotor region. *J Comp Neurol*. 517:783-807.
- Stepniewska I, Fang PC, Kaas JH. 2005. Microstimulation reveals specialized subregions for different complex movements in posterior parietal cortex of prosimian galagos. *Proc Natl Acad Sci U S A*. 102:4878-4883.
- Stepniewska I, Preuss TM, Kaas JH. 1993. Architectonics, somatotopic organization, and ipsilateral cortical connections of the primary motor area (M1) of owl monkeys. *J Comp Neurol*. 330:238-271.
- Steppan SJ, Storz BL, Hoffmann RS. 2004. Nuclear DNA phylogeny of the squirrels (Mammalia: Rodentia) and the evolution of arboreality from c-myc and RAG1. *Mol Phylogenet Evol*. 30:703-719.
- Sur M, Nelson RJ, Kaas JH. 1978. The representation of the body surface in somatosensory area I of the grey squirrel. *J Comp Neurol*. 179:425-450.
- Tandon S, Kambi N, Jain N. 2008. Overlapping representations of the neck and whiskers in the rat motor cortex revealed by mapping at different anaesthetic depths. *Eur J Neurosci*. 27:228-237.
- Tennant KA, Adkins DL, Donlan NA, Asay AL, Thomas N, Kleim JA, Jones TA. 2011. The organization of the forelimb representation of the C57BL/6 mouse motor cortex as defined by intracortical microstimulation and cytoarchitecture. *Cereb Cortex*. 21:865-876.
- Veenman C, Reiner A, Honig M. 1992. Biotinylated dextran amine as an anterograde tracer for single- and double-label studies. *J Neurosci Methods*. 41:239-254.
- Vincent SB. 1912. The functions of the vibrissae in the behavior of the white rat. *Behav Monogr*. 1:7-81.
- Wang Q, Burkhalter A. 2007. Area map of mouse visual cortex. *J Comp Neurol*. 502:339-357.
- Wang X, Zhang M, Cohen IS, Goldberg ME. 2007. The proprioceptive representation of eye position in monkey primary somatosensory cortex. *Nat Neurosci*. 10:640-646.
- Wong P, Kaas JH. 2008. Architectonic subdivisions of neocortex in the gray squirrel (*Sciurus carolinensis*). *Anat Rec (Hoboken)*. 291:1301-1333.
- Wong P, Kaas JH. 2009. Architectonic subdivisions of neocortex in the tree shrew (*Tupaia belangeri*). *Anat Rec (Hoboken)*. 292:994-1027.